

Popcorn-shaped polyethylene synthesised using highly active supported permethylindenyl metallocene catalyst systems

Jean-Charles Buffet, Zoë R. Turner, and Dermot O'Hare

Chemistry Research Laboratory, University of Oxford, 12 Mansfield Road, OX1 3TA, Oxford, UK.

Table of contents

1. General details and instrumentation	S2
2. Experimental details	S4
2.1 Complex synthesis	S4
2.2 Solid catalyst synthesis and polymerisation	S6
3. X-ray crystallography	S8
3.1 Tables	S8
3.2 Molecular structure illustrations	S11
4. NMR spectroscopy	S17
4.1 Solution NMR spectroscopy of complexes	S17
4.2 Solid state NMR spectroscopy of solid catalysts	S22
5. Polymerisation study	S29
5.1 Solution phase polymerisation	S29
5.2 SSMAO based slurry phase polymerisation	S31
5.3 LDHMAO based slurry phase polymerisation	S33
5.4 Solid MAO based slurry phase polymerisation	S36
5.5 Molecular weights	S39
6. References	S42

1. General details and instrumentation

General procedures. All reactions, unless specified otherwise, were performed under an atmosphere of nitrogen, using standard Schlenk techniques on a dual vacuum/inert gas manifold or within an MBraun UNILab glovebox. All glassware was placed in an oven at 160 °C for at least four hours prior to use.

Pentane, hexanes and benzene were dried using an MBraun SPS-800 solvent purification system and degassed prior to use. The solvents were stored in ampoules over a potassium mirror. Tetrahydrofuran was distilled from purple sodium/benzophenone ketyl radical and stored on molecular sieves. Benzene-*d*₆ was dried over Na/K. Chloroform-*d*₁ and pyridine-*d*₅ were dried over calcium hydride. All deuterated solvents were vacuum transferred and freeze-pump-thaw degassed three times prior to use. Molecular sieves (3 Å, 8–12 mesh) were baked at 140 °C under vacuum (< 10⁻² mbar) for at least 48 hours before use.

ZrCl₄ was supplied by Sigma Aldrich and dried at 140 °C overnight under vacuum (10⁻² mbar).

X-ray crystallography. Crystals were mounted on MiTeGen Micromounts with a perfluoropolyether oil (Fomblin YR1800, Alfa Aesar) and cooled rapidly to 150(1) K using an Oxford Cryosystems Cryostream unit.¹ Two different diffractometer setups were used as follows:

- i. An Enraf-Nonius Kappa CCD diffractometer using graphite monochromated Mo Kα radiation ($\lambda = 0.71073 \text{ \AA}$). Raw frame data were reduced using the DENZO-SMN package,² and corrected for absorption using SORTAV.³ Intensity data were collected using a multi-scan method with SCALEPACK (within DENZO-SMN).
- ii. An Oxford Diffraction Supernova using multilayer, orthogonal, micro-focus Cu Kα radiation ($\lambda = 1.5405 \text{ \AA}$). Raw frame data were collected, reduced and processed using CrysAlisPro.

The structures were solved using either direct methods with SIR-92,⁵ or using charge-flipping with SuperFlip,⁶ and refined using a full-matrix least squares refinement on all F² data using the CRYSTALS⁷ or Win-GX program suite.⁸ Dihedral angles were calculated with CCDC's Mercury⁹ or using PLATON.¹⁰ Illustrations of the solid-state molecular structures were created using ORTEP-3.¹¹

Solution phase NMR spectroscopy. All air- and moisture-sensitive compounds were prepared in a glovebox under a nitrogen atmosphere, using dried solvents and sealed in 5 mm Young's type NMR tubes. Spectra were recorded at 298 K on a Bruker AVIII 400 MHz NMR spectrometer. ¹H and ¹³C NMR spectra were referenced internally to the residual *proto*-solvent resonance. ¹H and ¹³C{¹H} chemical shifts, δ , are given in parts per million (ppm) relative to tetramethylsilane ($\delta = 0$).

Solid-state NMR spectroscopy. All samples were prepared in a glovebox under a nitrogen atmosphere and sealed in 4 mm ZrO₂ rotors. Solid-state NMR spectra were recorded by Dr. Nicholas Rees (University of Oxford), on a Bruker AVIII HD NanoBay 400 MHz Solid-State NMR spectrometer. Samples were spun at the magic angle (54.71°) at spin rates of 10 kHz for ¹³C, ²⁷Al and ²⁹Si CPMAS, and ²⁹Si DPMAS NMR. ¹³C CPMAS NMR spectra were acquired with a cross-polarisation sequence with a variable X-amplitude spin-lock pulse and phase modulated proton decoupling was used. 13,000 transients were acquired using a contact time of 1 ms, an acquisition time of 41 ms (1024 data points zero filled to 16 K) and a recycle delay of 30 s. All ¹³C spectra were referenced to adamantane (the upfield methine resonance was taken to be at $\delta = 29.5$ ppm on a scale where $\delta(\text{TMS}) = 0$) as a secondary reference. ²⁷Al MAS NMR spectra were acquired with a single

pulse excitation using a short pulse length (0.7 μ s). Each spectrum resulted from 2000 scans separated by a 1 s delay. The ^{27}Al chemical shifts are referenced to an aqueous solution of $\text{Al}(\text{NO}_3)_3$ ($\delta = 0$ ppm). ^{29}Si DPMAS NMR spectra were acquired with an acquisition time of 68 ms (1024 data points zero filled to 16 K) and a recycle delay of 30 s. All ^{29}Si spectra were externally referenced to kaolinite (taken to be at $\delta = -91.7$ ppm on a scale where $\delta(\text{TMS}) = 0$) as a secondary reference.

Scanning electron microscopy. Scanning electron microscopy (SEM) images were collected by Mr Phakpoom Angpanitcharoen and Miss Jessica Lamb (University of Oxford), on a JEOL JSM 6610 scanning electron microscope. Particles were cast onto a silica wafer. Before imaging, the samples were coated with platinum to prevent charging, improving the image quality. Energy dispersive X-ray (EDX) spectroscopy was also performed on this instrument to determine the relative percentages of elements on the surface.

Gel permeation chromatography. Gel permeation chromatography (GPC) samples were collected by Mrs Liv Thorbu at Norner AS, Norway on a high temperature gel permeation chromatograph with a IR5 infrared detector (GPC-IR5). Samples were prepared by dissolution in 1,2,4-trichlorobenzene (TCB) containing 300 ppm of 3,5-di-*tert*-butyl-4-hydroxytoluene (BHT) at 160 °C for 90 minutes and then filtered with a 10 μm SS filter before being passed through the GPC column. The samples were run under a flow rate of 0.5 mL/min using TCB containing 300 ppm of BHT as mobile phase with 1 mg/mL BHT added as a flow rate marker. The GPC column and detector temperature were set at 145 °C and 160 °C respectively.

Inductively coupled plasma optical emission spectrometry. ICP-OES were carried out on an Agilent 5110 ICP-OES using aVistaChip II CCD detector by Prof. Vincenzo Busico (University of Naples).

2. Experimental details

2.1 Complex synthesis

The complex synthesis was carried out in a one pot synthesis over three steps. ^tBu₂FluLi (1 equivalent, bright yellow solid) was introduced into a Schlenk in a glove box and dissolved in tetrahydrofuran (40 mL) on a Schlenk line to afford a dark red solution. This solution was added dropwise (over 10 minutes) to a cold solution (5 °C) of ^{3-R}Ind*SiR₁R₂Cl (3 equivalents, orange oil/ low temperature melting solid) in tetrahydrofuran (10 mL, yellow solution). The reaction was warmed to room temperature after addition and stirred for 1 h.

The reaction mixture then was cooled to 5 °C and to this was added ⁿBuLi (2.2 equivalents, 2.5 M in hexanes) before being allowed to stir for 0.5 h at room temperature. The solution darkened from yellow to red over time. The solution was then dried and the dark red solid/oil was washed with pentane (3 × 50 mL) and dried again to afford a flaky orange solid of R₁R₂SB(^tBu₂Flu,^{3-R}I*)Li₂ in assumed quantitative yields as judged by ¹H NMR spectroscopy.

The dilithium salt, R₁R₂SB(^tBu₂Flu,^{3-R}I*)Li₂, (1 equivalent) was combined with ZrCl₄ (1 equivalent) in a Schlenk in a glovebox and benzene (50 mL) was added. The beige mixture was stirred, turning first pale- then dark orange, for 3 to 24 h at room temperature. The solid (beige) was left to settle and the solution (dark orange) was filtered away, concentrated and left either at room temperature or in a fridge (8 °C). If no crystals were obtained, the solution was dried and the orange solid was dissolved in a minimum of pentane, filtered and left in a freezer (-30 °C).

Me₂SB(^tBu₂Flu,I*)ZrCl₂ (1): orange crystals obtained from benzene solution at room temperature in 18% yield.

¹H NMR (C₆D₆, 400 MHz, 298 K): δ 1.19 (s, 9H, FluCMe₃), 1.26 (s, 3H, SiMe₂), 1.32 (s, 3H, SiMe₂), 1.35 (s, 9H, FluCMe₃), 2.01 (s, 3H, Ind*Me), 2.03 (s, 3H, Ind*Me), 2.14 (s, 3H, Ind*Me), 2.34 (s, 3H, Ind*Me), 2.41 (s, 3H, Ind*Me), 2.62 (s, 3H, Ind*Me), 7.45 (s, 1H, FluH), 7.49 (dd, 2H, FluH), 7.72 (s, 1H, FluH) and 7.79 (dd, 2H, FluH).

¹³C{¹H} NMR (C₆D₆, 100 MHz, 298 K): 5.3 (SiMe₂), 8.8 (SiMe₂), 16.3 (Ind*Me), 16.4 (Ind*Me), 16.7 (Ind*Me), 17.8 (Ind*Me), 18.0 (Ind*Me), 22.6 (Ind*Me), 30.9 (FluCMe₃), 31.3 (FluCMe₃), 35.3 (FluCMe₃), 35.3 (FluCMe₃), 63.9 (SiFlu), 78.9 (SiInd*), 118.7 (FluCH), 121.2 (FluCH), 124.2 (FluCH), 124.4 (FluCH), 125.8 (FluCH), 125.8 (FluCH), 127.1 (FluAr), 128.6 (FluAr), 128.7 (FluAr), 129.5 (FluAr), 131.1 (Ind*Ar), 131.5 (Ind*Ar), 133.6 (Ind*Ar), 133.8 (Ind*Ar), 134.3 (Ind*Ar), 135.9 (Ind*Ar), 150.0 (FluAr) and 150.9 (FluAr).

Elemental analysis: calculated: C: 65.67, H: 6.96; found: C: 65.63, H: 7.06.

Et₂SB(^tBu₂Flu,I*)ZrCl₂ (2): orange crystals obtained from pentane solution at -30 °C in 8% yield.

¹H NMR (CDCl₃, 400 MHz, 298 K): δ 1.16 (s, 9H, FluCMe₃), 1.34 (s, 9H, FluCMe₃), 1.38 (m, 3H, SiCH₂Me), 1.55 (m, 3H, SiCH₂Me), 1.88 (m, 2H, SiCH₂Me), 2.11 (s, 6H, Ind*Me), 2.14 (m, 2H, SiCH₂Me), 2.17 (s, 3H, Ind*Me), 2.23 (s, 3H, Ind*Me), 2.34 (s, 3H, Ind*Me), 2.37 (s, 3H, Ind*Me), 2.64 (s, 3H, Ind*Me), 7.25 (s, 1H, FluH), 7.52 (dd, 2H, FluH), 7.56 (s, 1H, FluH) and 7.81 (dd, 2H, FluH).

$^{13}\text{C}\{\text{H}\}$ NMR (CDCl₃, 100 MHz, 298 K): 6.9 (SiCH₂Me), 7.7 (SiCH₂Me), 14.2 (Ind*Me), 16.2 (Ind*Me), 16.3 (Ind*Me), 16.3 (Ind*Me), 17.8 (Ind*Me), 17.8 (Ind*Me), 22.5 (SiCH₂Me), 22.5 (SiCH₂Me), 30.8 (FluCMe₃), 31.2 (FluCMe₃), 35.2 (FluCMe₃), 35.4 (FluCMe₃), 63.2 (SiFlu), 78.5 (SiInd*), 118.6 (FluCH), 121.2 (FluCH), 123.6 (FluCH), 123.8 (FluCH), 125.5 (FluCH), 125.6 (FluCH), 126.8 (FluAr), 127.9 (FluAr), 128.1 (FluAr), 128.2 (FluAr), 131.1 (Ind*Ar), 131.2 (Ind*Ar), 133.7 (Ind*Ar), 134.2 (Ind*Ar), 134.6 (Ind*Ar), 136.7 (Ind*Ar), 150.3 (FluAr) and 151.1 (FluAr).

Elemental analysis: calculated: C: 66.44, H: 7.25; found: C: 66.24, H: 7.05.

MePropSB(^tBu₂Flu,I*)ZrCl₂ (3): orange crystals obtained from benzene solution at room temperature in less than 2% yield.

^1H NMR (CDCl₃, 400 MHz, 298 K): δ 1.16 (s, 9H, FluCMe₃), 1.18 (s, 9H, FluCMe₃), 1.33 (m, 6H, SiCH₂CH₂Me), 1.34 (s, 9H, FluCMe₃), 1.35 (s, 9H, FluCMe₃), 1.48 (s, 3H, SiMe), 1.49 (s, 3H, SiMe), 1.89 (m, 6H, SiCH₂CH₂Me), 2.10 (s, 9H, Ind*Me), 2.11 (s, 3H, Ind*Me), 2.17 (s, 6H, Ind*Me), 2.33 (s, 3H, Ind*Me), 2.34 (s, 6H, Ind*Me), 2.36 (s, 3H, Ind*Me), 2.38 (s, 6H, Ind*Me), 2.66 (s, 6H, Ind*Me), 7.30 (s, 2H, FluH), 7.54 (dd, 4H, FluH), 7.59 (s, 2H, FluH), and 7.82 (dd, 2H, FluH).

$^{13}\text{C}\{\text{H}\}$ NMR (CDCl₃, 100 MHz, 298 K): 2.6 (SiMe), 5.8 (SiMe), 14.2 (2 × SiCH₂CH₂Me), 16.2 (Ind*Me), 16.3 (Ind*Me), 16.3 (Ind*Me), 16.3 (Ind*Me), 16.8 (Ind*Me), 17.3 (SiCH₂CH₂Me), 17.7 (Ind*Me), 17.8 (Ind*Me), 17.8 (Ind*Me), 17.8 (Ind*Me), 18.7 (Ind*Me), 22.5 (Ind*Me), 22.6 (Ind*Me), 22.7 (SiCH₂CH₂Me), 22.7 (SiCH₂CH₂Me), 30.8 (FluCMe₃), 30.9 (FluCMe₃), 31.2 (FluCMe₃), 31.2 (FluCMe₃), 35.2 (FluCMe₃), 35.2 (FluCMe₃), 35.4 (FluCMe₃), 35.4 (FluCMe₃), 63.7 (2 × SiFlu), 78.4 (2 × SiInd*), 118.6 (FluCH), 121.2 (FluCH), 123.6 (FluCH), 123.7 (FluCH), 123.8 (FluCH), 125.4 (FluCH), 125.6 (FluCH), 125.7 (FluCH), 126.9 (FluCH), 127.0 (FluCH), 127.7 (FluCH), 127.8 (FluCH), 127.8 (FluAr), 128.0 (FluAr), 128.2 (FluAr), 128.2 (FluAr), 128.3 (FluAr), 128.7 (FluAr), 128.7 (FluAr), 129.0 (FluAr), 131.1 (2 × Ind*Ar), 132.0 (Ind*Ar), 132.8 (Ind*Ar), 133.7 (Ind*Ar), 133.7 (Ind*Ar), 133.9 (Ind*Ar), 134.0 (Ind*Ar), 134.2 (Ind*Ar), 134.5 (Ind*Ar), 134.6 (Ind*Ar), 134.9 (Ind*Ar), 150.2 (FluAr) and 151.1 (FluAr).

Me₂SB(^tBu₂Flu,³-EtI*)ZrCl₂ (4): orange crystals obtained from benzene solution at room temperature in 9% yield.

^1H NMR (CDCl₃, 400 MHz, 298 K): δ 0.92 (s, 3H, Ind*CH₂Me), 1.17 (s, 9H, FluCMe₃), 1.34 (s, 9H, FluCMe₃), 1.46 (s, 3H, SiMe₂), 1.49 (s, 3H, SiMe₂), 2.12 (s, 6H, Ind*Me), 2.21 (s, 3H, Ind*Me), 2.35 (s, 3H, Ind*Me), 2.55 (s, 1H, Ind*CH₂Me), 2.69 (s, 3H, Ind*Me), 3.04 (s, 1H, Ind*CH₂Me), 7.30 (s, 1H, FluH), 7.53 (dd, 2H, FluH), 7.61 (s, 1H, FluH) and 7.80 (dd, 2H, FluH).

$^{13}\text{C}\{\text{H}\}$ NMR (CDCl₃, 100 MHz, 298 K): 5.5 (SiMe₂), 8.9 (SiMe₂), 15.0 (Ind*CH₂Me), 15.9(Ind*Me), 16.5 (Ind*Me), 16.7 (Ind*Me), 17.9 (Ind*Me), 22.6 (Ind*Me), 22.9 (Ind*CH₂Me), 30.8 (FluCMe₃), 31.2 (FluCMe₃), 35.2 (FluCMe₃), 35.34 (FluCMe₃), 63.8 (SiFlu), 79.3 (SiInd*), 118.5 (FluCH), 121.0 (FluCH), 123.6 (FluCH), 123.8 (FluCH), 125.6 (FluCH), 125.7 (FluCH), 127.3 (FluAr), 127.7 (FluAr), 128.2 (FluAr), 130.6 (FluAr), 130.8 (Ind*Ar), 132.7 (Ind*Ar), 133.6 (Ind*Ar), 133.8 (Ind*Ar), 134.4 (Ind*Ar), 136.0 (Ind*Ar), 150.1 (FluAr) and 151.0 (FluAr).

Elemental analysis: calculated: C: 66.07, H: 7.11; found: C: 66.27, H: 6.97.

Me₂SB(tBu₂Flu,I*)HfCl₂ (5): orange crystals obtained from benzene solution at room temperature in less than 2% yield.

¹H NMR (C₆D₆, 400 MHz, 298 K): δ 1.20 (s, 9H, FluCMe₃), 1.28 (s, 3H, SiMe₂), 1.29 (s, 3H, SiMe₂), 1.37 (s, 9H, FluCMe₃), 2.03 (s, 3H, Ind*Me), 2.07 (s, 3H, Ind*Me), 2.29 (s, 3H, Ind*Me), 2.32 (s, 3H, Ind*Me), 2.45 (s, 3H, Ind*Me), 2.64 (s, 3H, Ind*Me), 7.41 (s, 1H, FluH), 7.50 (dd, 2H, FluH), 7.78 (dd, 2H, FluH) and 7.79 (s, 1H, FluH).

¹³C{¹H} NMR (C₆D₆, 100 MHz, 298 K): 5.2 (SiMe₂), 8.5 (SiMe₂), 16.2 (Ind*Me), 16.2 (Ind*Me), 16.5 (Ind*Me), 17.8 (Ind*Me), 18.0 (Ind*Me), 22.7 (Ind*Me), 30.9 (FluCMe₃), 31.4 (FluCMe₃), 35.2 (FluCMe₃), 35.3 (FluCMe₃), 62.9 (SiFlu), 81.11 (SiInd*), 118.64 (FluCH), 120.71 (FluCH), 123.65 (FluCH), 124.04 (FluCH), 125.0 (FluCH), 125.6 (FluCH), 127.1 (FluAr), 129.0 (FluAr), 129.2 (FluAr), 126.9 (FluAr) 131.2 (Ind*Ar), 131.3 (Ind*Ar), 132.0 (Ind*Ar), 133.4 (Ind*Ar), 134.1 (Ind*Ar), 134.3 (Ind*Ar), 149.6 (FluAr) and 150.7 (FluAr).

2.2 Solid catalyst synthesis and polymerisation

Synthesis of solid catalysts. The quantity of catalyst immobilised on the surface of the support is given in terms of the M:Zr ratio of the methylalumininoxane (MAO) component to the organometallic complex. In the case of SSMAO and LDHMAO, 40wt% MAO was used to activate the surface of each support. The M:Zr ratio used in this work is 200:1. The molecular weights used for SiO₂ and LDH ($Mg_{0.75}Al_{0.25}(OH)_2(CO_3)_{0.125}$) are 59.97 and 70.73 g.mol⁻¹ respectively. This gives rise to molecular masses of SSMAO and LDHMAO of 177.94 and 199.46 g.mol⁻¹. SSMAO and LDHMAO are prepared by weighing out silica or LDH and MAO into a Schlenk in a glovebox and then adding toluene (40 mL) to the mixture, heating at 80 °C for 2 h with regular swirling and then drying under vacuum (1×10^{-2} mbar) at room temperature for at least 4 h to ensure all the solvent was removed.

Solid polymethylalumininoxane (solid MAO or sMAO) was synthesised according to literature procedure.^{13,14}

The finished solid catalysts were synthesised according to the following method: in a glove box, the inorganic support (SSMAO, LDHMAO or sMAO) and the desired complex were weighed into a Schlenk in a [Al_{MAO}]₀:[M_{complex}]₀ of 200:1 ratio. Then, toluene (40 mL) was added and the slurry was heated at 60 °C for 1 h with regular swirling. The coloured solid was allowed to settle, then the colourless solution was decanted (or filtered), and the product dried under vacuum (1×10^{-2} mbar) at room temperature for at least 4 h to ensure all the solvent was removed and afforded in 73–92% isolated yields.

SSMAO-Me₂SB(tBu₂Flu,I*)ZrCl₂ (1_{SSMAO}): light purple solid in 88% isolated yield.

²⁹Si CPMAS NMR: δ -103 (SiO₂), -23, -16, -7 and 23 (SiMe₂).

²⁷Al DPMAS hahn echo NMR: δ -92 (m, AlOMe).

¹³C CPMAS NMR: δ -8.67 (AlOMe), 13.09 (SiMe₂), 24.20 (Ar-Me), 29.18 (Ar-Me), 34.52 (Ar-Me), 70–80 (SiInd*/Si-Flu), 121–140 (FluCH), 140–150 (FluAr).

SSMAO-Me₂SB(tBu₂Flu,I*)HfCl₂ (5_{SSMAO}): dark pink solid in 78% isolated yield.

LDHMAO-Me₂SB(tBu₂Flu,I*)ZrCl₂ (1_{LDHMAO}): pale pink solid in quantitative yield.

²⁹Si CPMAS NMR: δ -23 and -7 (*SiMe₂*).

²⁷Al DPMAS NMR: δ 8 (Mg*Al*-CO₃) and 65 (*AlOMe*).

²⁷Al DPMAS hahnecho NMR: δ -92 (m, Mg*Al*-CO₃/ *AlOMe*).

LDHMAO-Et₂SB(tBu₂Flu,I*)ZrCl₂ (2_{LDHMAO}): pale pink solid in 73% isolated yield.

LDHMAO-Me₂SB(tBu₂Flu,I*)HfCl₂ (5_{LDHMAO}): purple solid in 85% isolated yield.

sMAO-Me₂SB(tBu₂Flu,I*)ZrCl₂ (1_{sMAO}): peach solid in 92% isolated yield.

ICP-OES (expected: [Al_{sMAO}]₀/[Zr_{complex}]₀: 200, found: [Al_{sMAO}]₀/[Zr_{complex}]₀: 160; Zr wt%: 0.70 and Al wt%: 38.2.

²⁹Si CPMAS NMR: δ -16 (*SiMe₂*).

²⁷Al DPMAS NMR: δ 11 (m, *Al* in sMAO).

¹³C CPMAS NMR: δ -8.20 (*AlOMe*), 15.87 (*SiMe₂*), 30.05 (Ar-*Me*), 128 (*FluCH*), 135 (*FluAr*).

sMAO-Et₂SB(tBu₂Flu,I*)ZrCl₂ (2_{sMAO}): peach solid in 79% isolated yield.

ICP-OES (expected: [Al_{sMAO}]₀/[Zr_{complex}]₀: 200, found: [Al_{sMAO}]₀/[Zr_{complex}]₀: 185; Zr wt%: 0.70 and Al wt%: 38.2.

²⁷Al DPMAS NMR: δ 11 (m, *Al* in sMAO).

²⁷Al DPMAS hahnecho NMR: δ -92 (m, *Al* in sMAO).

¹³C CPMAS NMR: δ -8.26 (*AlOMe*), 24.07 (Ar-*Me*), 49.49, 70-80 (*SiInd**/*Si-Flu*), 128 (*FluCH*), 135 (*FluAr*).

sMAO-MePropSB(tBu₂Flu,I*)ZrCl₂ (3_{sMAO}): peach solid in 91% isolated yield.

ICP-OES (expected: [Al_{sMAO}]₀/[Zr_{complex}]₀: 200, found: [Al_{sMAO}]₀/[Zr_{complex}]₀: 211; Zr wt%: 0.77 and Al wt%: 36.5.

sMAO-Me₂SB(tBu₂Flu,³-EtI*)ZrCl₂ (4_{sMAO}): peach solid in 83% isolated yield.

ICP-OES (expected: [Al_{sMAO}]₀/[Zr_{complex}]₀: 200, found: [Al_{sMAO}]₀/[Zr_{complex}]₀: 208; Zr wt%: 0.60 and Al wt%: 37.0.

sMAO-Me₂SB(tBu₂Flu,I*)HfCl₂ (5_{sMAO}): pink solid in 91% isolated yield.

ICP-OES (expected: [Al_{sMAO}]₀/[Hf_{complex}]₀: 200, found: [Al_{sMAO}]₀/[Hf_{complex}]₀: 203; Hf wt%: 1.12 and Al wt%: 34.4.

Slurry phase ethylene polymerisation studies. A typical slurry-phase laboratory polymerisation run was performed as follows. 150 mg triisobutylaluminium (TIBA) was

added into a vial and 10 mL of hexanes was added. This mixture was introduced into a 150 mL Rotaflow ampoule containing a stirrer bar and swirled around the glassware. 10 mg supported catalyst was added to the ampoule and washed in with a further 40 mL hexanes. The vessel was sealed and was pumped on to a vacuum line and degassed under reduced pressure. It was cycled a further three times using an ethylene purge while the reaction was brought to temperature in an oil bath with the stirring was set at 1000 rpm. The stopcock was opened to ethylene at a pressure of 2 bar and the timer was started. On completion of the run, the vessel was closed to ethylene and degassed, then filtered on a glass sintered frit (porosity 3) and washed with 2 × 25 mL pentane. The polyethylene (PE) was dried in vacuum until constant weight. All polymerisation runs were carried out at least twice to ensure reproducibility.

Solution phase ethylene polymerisation studies. A stock solution of a complex in toluene was prepared at a concentration of 0.2 mg/mL. 2000 equivalents MAO were added to a 150 ml Rotaflow ampoule and washed in with 9 mL hexanes. 1 ml stock solution was added to the ampoule along with a further 40 mL hexanes. The run was continued as above.

3. X-ray crystallography

3.1 Tables

Table S1: Selected bond lengths (\AA) and angles ($^\circ$).

	(1)	(2)	(3)	(4)	(5)
M(1)-Cp _{cent} (Ind)	2.227	2.233	2.228	2.235	2.205
M(1)-Cp _{cent} (Flu)	2.300	2.305	2.307	2.316	2.293
M(1)-C(1)	2.468(3)	2.4933(19)	2.496(4)	2.4690(18)	2.458(3)
M(1)-C(18)	2.422(3)	2.3936(19)	2.390(4)	2.4161(19)	2.395(3)
M(1)-Cl(1)	2.4189(9)	2.4193(5)	2.4243(10)	2.4186(5)	2.3906(7)
M(1)-Cl(2)	2.4120(9)	2.4148(5)	2.4164(11)	2.4041(5)	2.3862(7)
Si(1)-C(1)	1.913(4)	1.912(2)	1.914(5)	1.909(2)	1.909(3)
Si(1)-C(18)	1.877(3)	1.870(2)	1.867(4)	1.874(2)	1.877(3)
C(1)-Si(1)-C(18)	95.61(15)	95.42(8)	95.69(18)	95.53(8)	95.18(13)
Cl(1)-M(1)-Cl(2)	97.18(3)	96.156(19)	97.82(4)	97.796(19)	96.38(3)
α	62.04	62.07	62.35	63.63	62.00

α : angle formed between Cp(Ind) and Cp(Flu) planes

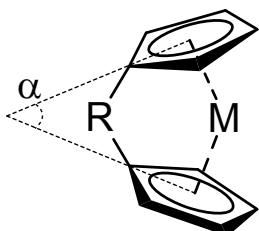


Table S2: Selected experimental crystallographic data.

Complex	$\text{Me}_2\text{SB}(\text{tBu}_2\text{Flu}, \text{I}^*)\text{H}_2$	$\text{Me}_2\text{SB}(\text{tBu}_2\text{Flu}, \text{I}^*)\text{ZrCl}_2$ (1)	$\text{Et}_2\text{SB}(\text{tBu}_2\text{Flu}, \text{I}^*)\text{ZrCl}_2$ (2)
Chemical formula	$\text{C}_{38}\text{H}_{50}\text{Si}$	$\text{C}_{38}\text{H}_{48}\text{Cl}_2\text{SiZr}\cdot\text{C}_6\text{H}_6$	$2(\text{C}_{40}\text{H}_{52}\text{Cl}_2\text{SiZr})\cdot\text{C}_5\text{H}_{12}$
M_r	534.87	773.08	1518.19
Crystal system, space group	Orthorhombic, $P2_12_12_1$	Triclinic, $P\bar{1}$	Triclinic, $P\bar{1}$
Temperature (K)	150	150	150
a, b, c (Å)	10.0265 (1), 12.7798 (1), 25.9558 (3)	10.5809 (3), 13.3793 (3), 14.5519 (5)	13.8066 (4), 15.6857 (5), 19.9468 (6)
α, β, γ (°)	90, 90, 90	94.719 (2), 106.544 (3), 94.233 (2)	78.658 (2), 76.378 (2), 69.286 (3)
V (Å ³)	3325.89 (6)	1957.84 (10)	3896.2 (2)
Z	4	2	2
Radiation type	Mo $K\alpha$	Cu $K\alpha$	Cu $K\alpha$
μ (mm ⁻¹)	0.09	4.06	4.07
Crystal size (mm)	0.46 × 0.34 × 0.32	0.10 × 0.05 × 0.04	0.05 × 0.04 × 0.03
Diffractometer	Nonius KappaCCD diffractometer	SuperNova, Dual, Cu at zero, Atlas diffractometer	SuperNova, Dual, Cu at zero, Atlas diffractometer
Absorption correction	Multi-scan <i>DENZO/SCALEPACK</i> (Otwinowski & Minor, 1997)	Multi-scan <i>CrysAlis PRO</i> 1.171.38.41 (Rigaku Oxford Diffraction, 2015) Empirical absorption correction using SCALE3 ABSPACK.	Multi-scan <i>CrysAlis PRO</i> , Agilent Technologies, Version 1.171.35.21 (release 20-01-2012 CrysAlis171.NET) (compiled Jan 23 2012, 18:06:46) Empirical absorption correction using SCALE3 ABSPACK
T_{\min}, T_{\max}	0.91, 0.97	0.906, 1.000	0.872, 1.000
No. of measured, independent and observed [$I > 2\sigma(I)$] reflections	69900, 7565, 6119	13501, 7535, 6022	35708, 15963, 14154
R_{int}	-	0.039	0.022
$R[F^2 > 2\sigma(F^2)], wR(F^2), S$	0.048, 0.126, 1.02	0.039, 0.097, 1.13	0.030, 0.078, 1.03
No. of reflections	7565	7535	15963
No. of parameters	367	478	866
No. of restraints	0	96	28

Table S3: Selected experimental crystallographic data.

Complex	$\text{MePropSB}(\text{tBu}_2\text{Flu}, \text{I}^*)\text{ZrCl}_2$ (3)	$\text{Me}_2\text{SB}(\text{tBu}_2\text{Flu}, {}^3\text{-EtI}^*)\text{ZrCl}_2$ (4)	$\text{Me}_2\text{SB}(\text{tBu}_2\text{Flu}, \text{I}^*)\text{HfCl}_2$ (5)
Chemical formula	$\text{C}_{40}\text{H}_{52}\text{Cl}_2\text{SiZr}$	$\text{C}_{39}\text{H}_{50}\text{Cl}_2\text{SiZr}$	$\text{C}_{38}\text{H}_{48}\text{Cl}_2\text{HfSi}\cdot\text{C}_6\text{H}_6$
M_r	723.02	709.00	860.35
Crystal system, space group	Triclinic, $P\bar{1}$	Triclinic, $P\bar{1}$	Triclinic, $P\bar{1}$
Temperature (K)	150	150	150
a, b, c (Å)	15.4588 (8), 16.8913 (10), 19.2243 (9)	11.1926 (6), 12.9453 (7), 13.5301 (7)	10.5667 (4), 13.3377 (6), 14.5723 (7)
α, β, γ (°)	68.923 (5), 84.784 (4), 65.752 (5)	101.807 (4), 108.951 (5), 97.086 (4)	94.961 (4), 106.587 (4), 94.008 (4)
V (Å ³)	4261.2 (4)	1776.35 (17)	1951.27 (15)
Z	4	2	2
Radiation type	$\text{Cu K}\alpha$	$\text{Cu K}\alpha$	$\text{Cu K}\alpha$
μ (mm ⁻¹)	3.70	4.42	6.71
Crystal size (mm)	$0.21 \times 0.14 \times 0.02$	$0.04 \times 0.03 \times 0.03$	$0.11 \times 0.09 \times 0.08$
Diffractometer	SuperNova, Dual, Cu at zero, Atlas diffractometer	SuperNova, Dual, Cu at zero, Atlas diffractometer	SuperNova, Dual, Cu at zero, Atlas diffractometer
Absorption correction	Multi-scan <i>CrysAlis PRO</i> 1.171.38.41 (Rigaku Oxford Diffraction, 2015) Empirical absorption correction using SCALE3 ABSPACK	Multi-scan <i>CrysAlis PRO</i> , Agilent Technologies, Version 1.171.35.21 (release 20-01-2012) Empirical absorption correction using spherical harmonics, implemented in SCALE3 ABSPACK scaling algorithm.	Multi-scan <i>CrysAlis PRO</i> 1.171.38.41 (Rigaku Oxford Diffraction, 2015) Empirical absorption correction using SCALE3 ABSPACK.
T_{\min}, T_{\max}	0.704, 1.000	0.865, 1.000	0.920, 1.000
No. of measured, independent and observed [$I > 2\sigma(I)$] reflections	36995, 17380, 12177	14365, 7237, 6879	22260, 7762, 7228
R_{int}	0.058	0.027	0.024
$R[F^2 > 2\sigma(F^2)], wR(F^2), S$	0.050, 0.142, 1.06	0.033, 0.091, 0.96	0.029, 0.076, 1.07
No. of reflections	17380	7237	7762
No. of parameters	821	402	522
No. of restraints	0	0	145

3.2 Molecular structure illustrations

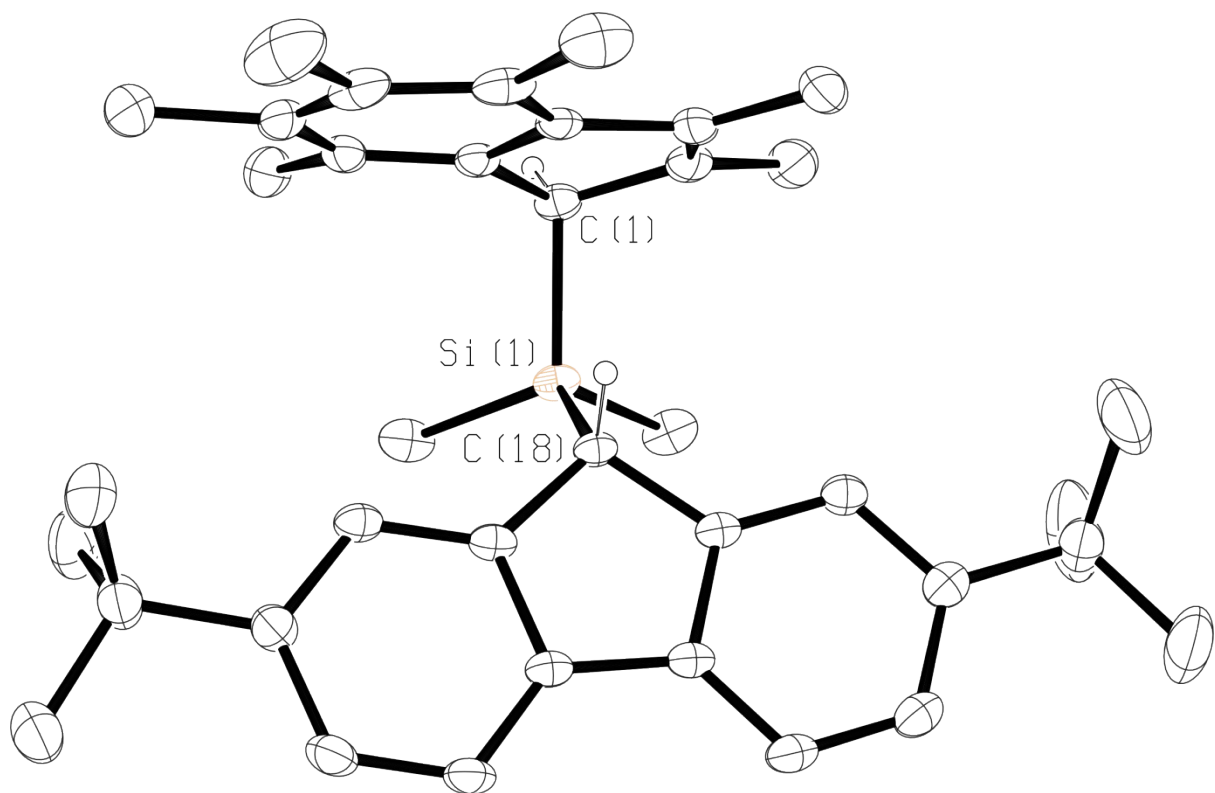


Fig. S1: Thermal displacement ellipsoid drawings (30% probability) of $^{Me_2}SB(^{t}Bu_2Flu,I^*)H_2$. All hydrogen atoms have been omitted for clarity (except for those attached to C1 and C18).

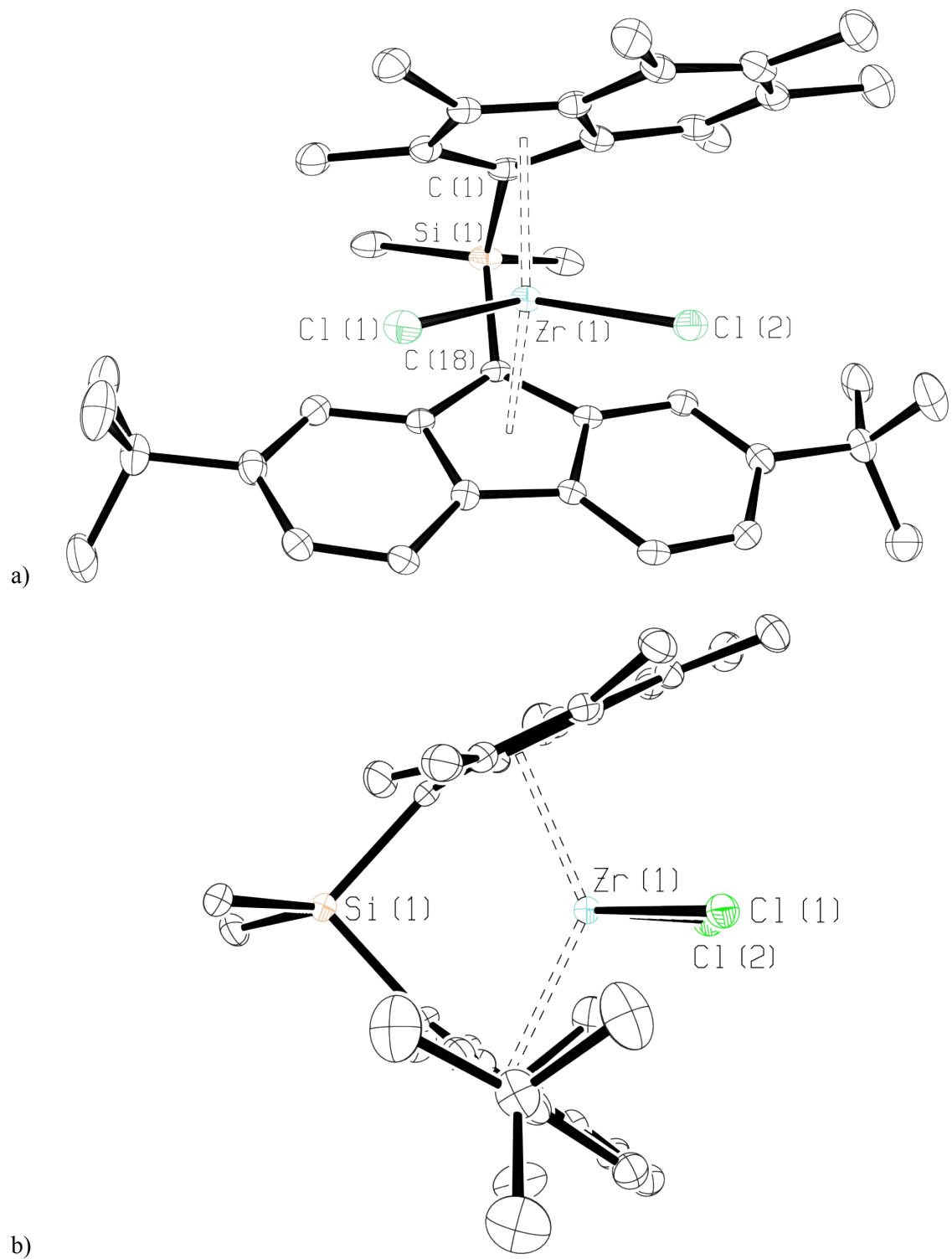


Fig. S2: Thermal displacement ellipsoid drawings (30% probability) of $\text{Me}_2\text{SB}(\text{tBu}_2\text{Flu}, \text{I}^*)\text{ZrCl}_2$ (**1**) a) front and b) side views. All hydrogen atoms have been omitted for clarity.

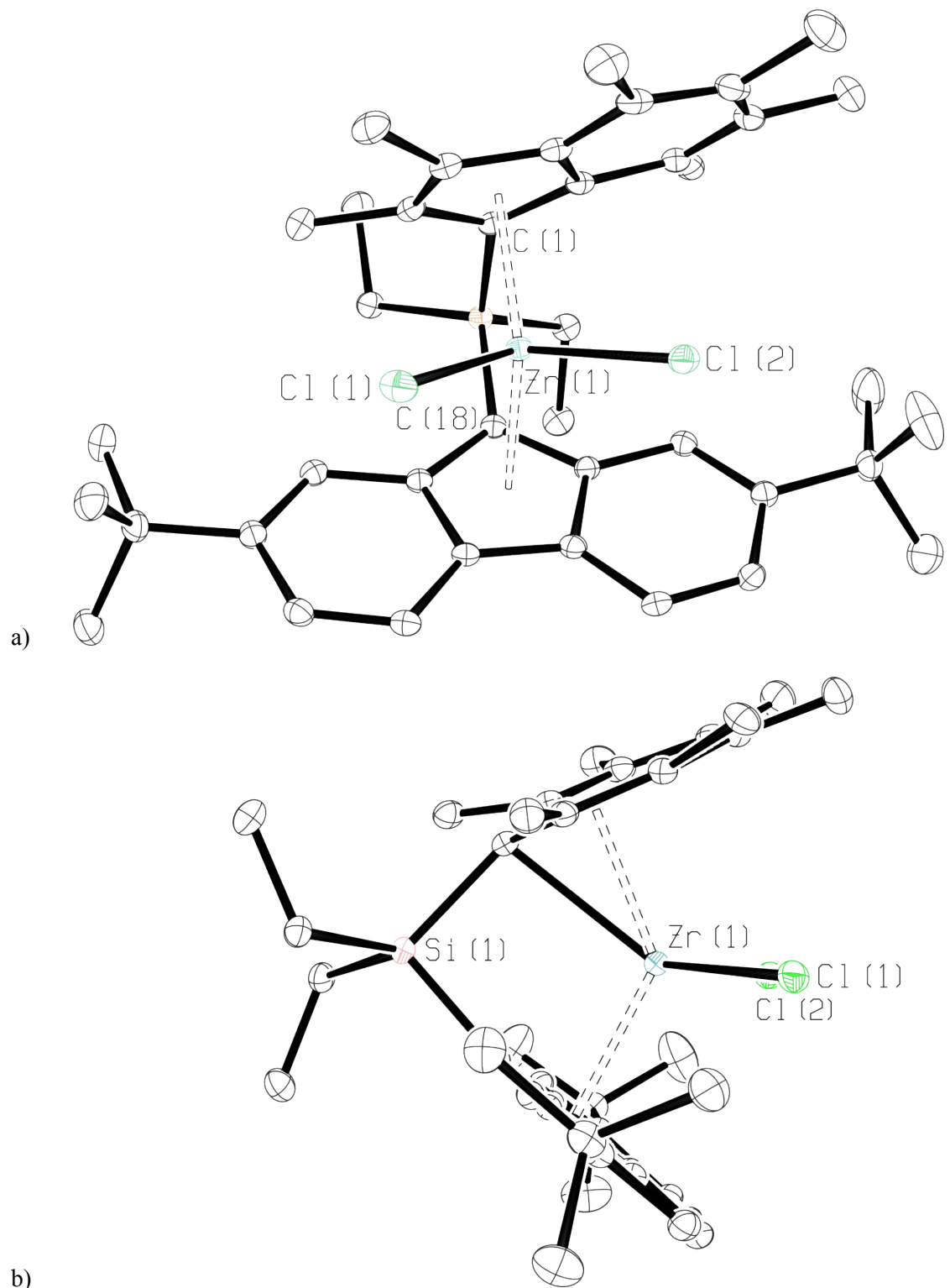


Fig. S3: Thermal displacement ellipsoid drawings (30% probability) of $\text{Et}_2\text{SB}(\text{tBu}_2\text{Flu}, \text{I}^*)\text{ZrCl}_2$ (2) a) front and b) side views. All hydrogen atoms have been omitted for clarity.

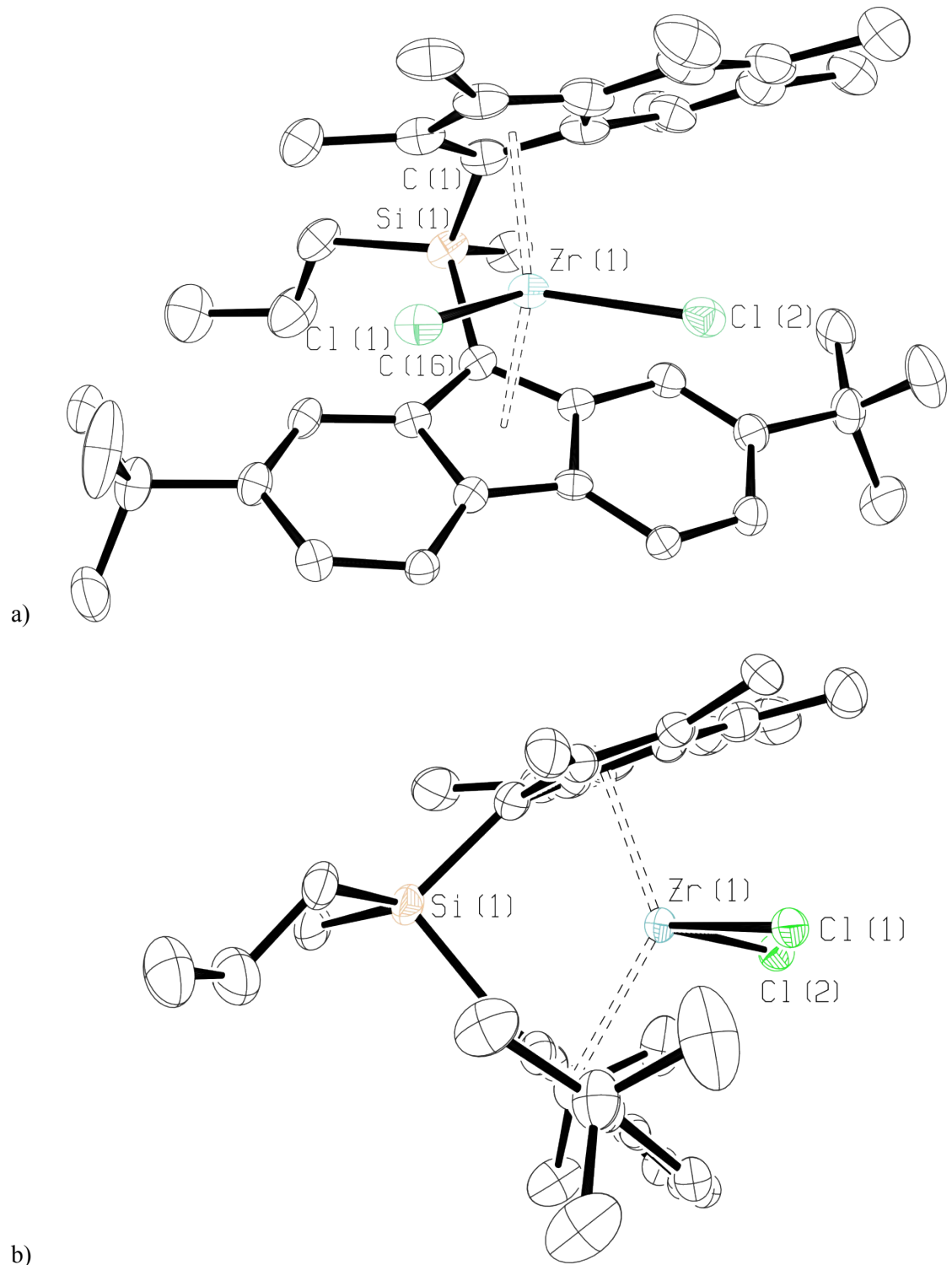


Fig. S4: Thermal displacement ellipsoid drawings (30% probability) of $^{MeProp}SB(^{tBu_2}Flu,I^*)ZrCl_2$ (**3**) a) front and b) side views. All hydrogen atoms have been omitted for clarity.

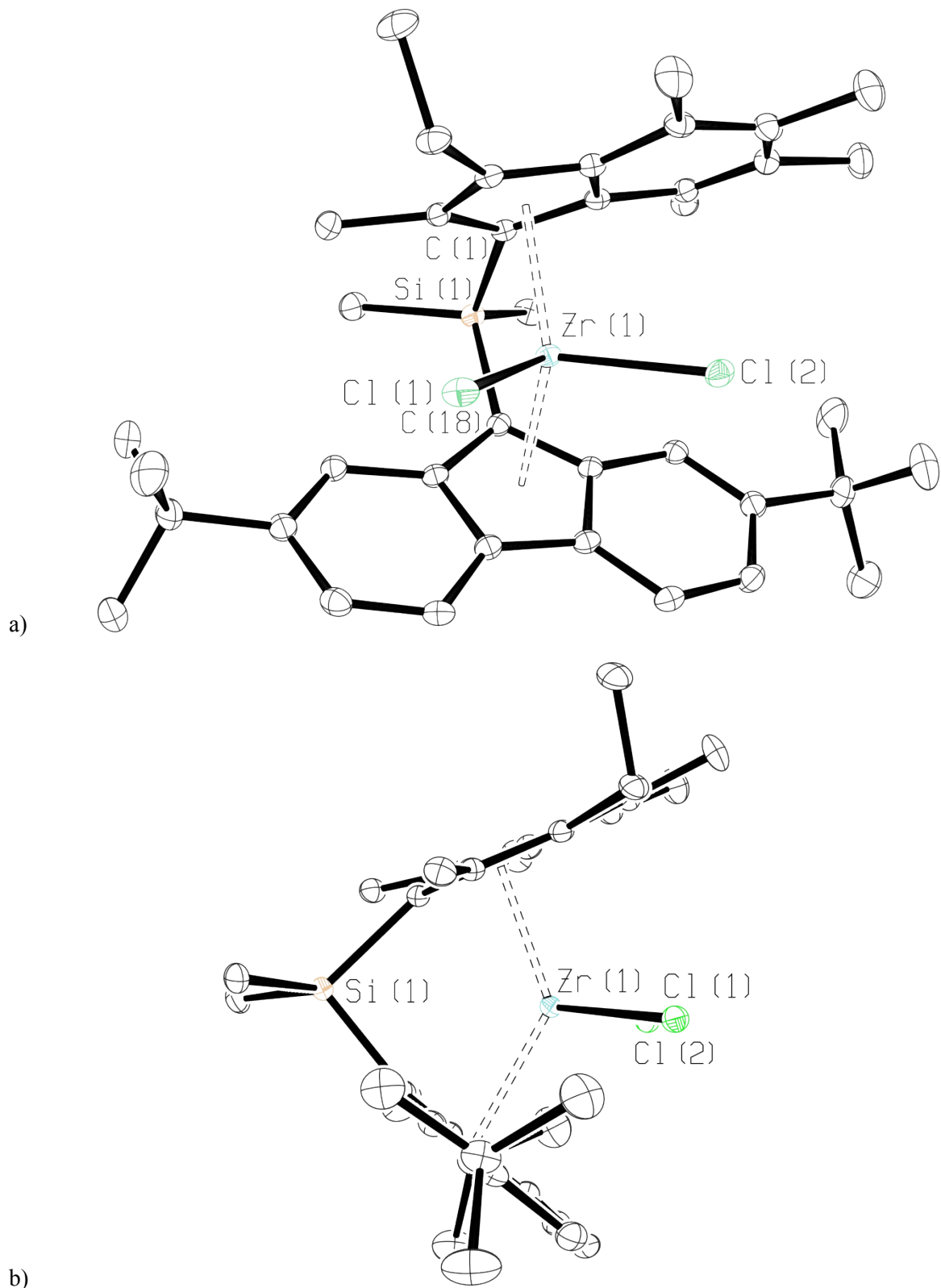


Fig. S5: Thermal displacement ellipsoid drawings (30% probability) of $\text{Me}_2\text{SB}(\text{tBu}_2\text{Flu}, {}^3\text{-EtI}^*)\text{ZrCl}_2$ (**4**)
a) front and b) side views. All hydrogen atoms have been omitted for clarity.

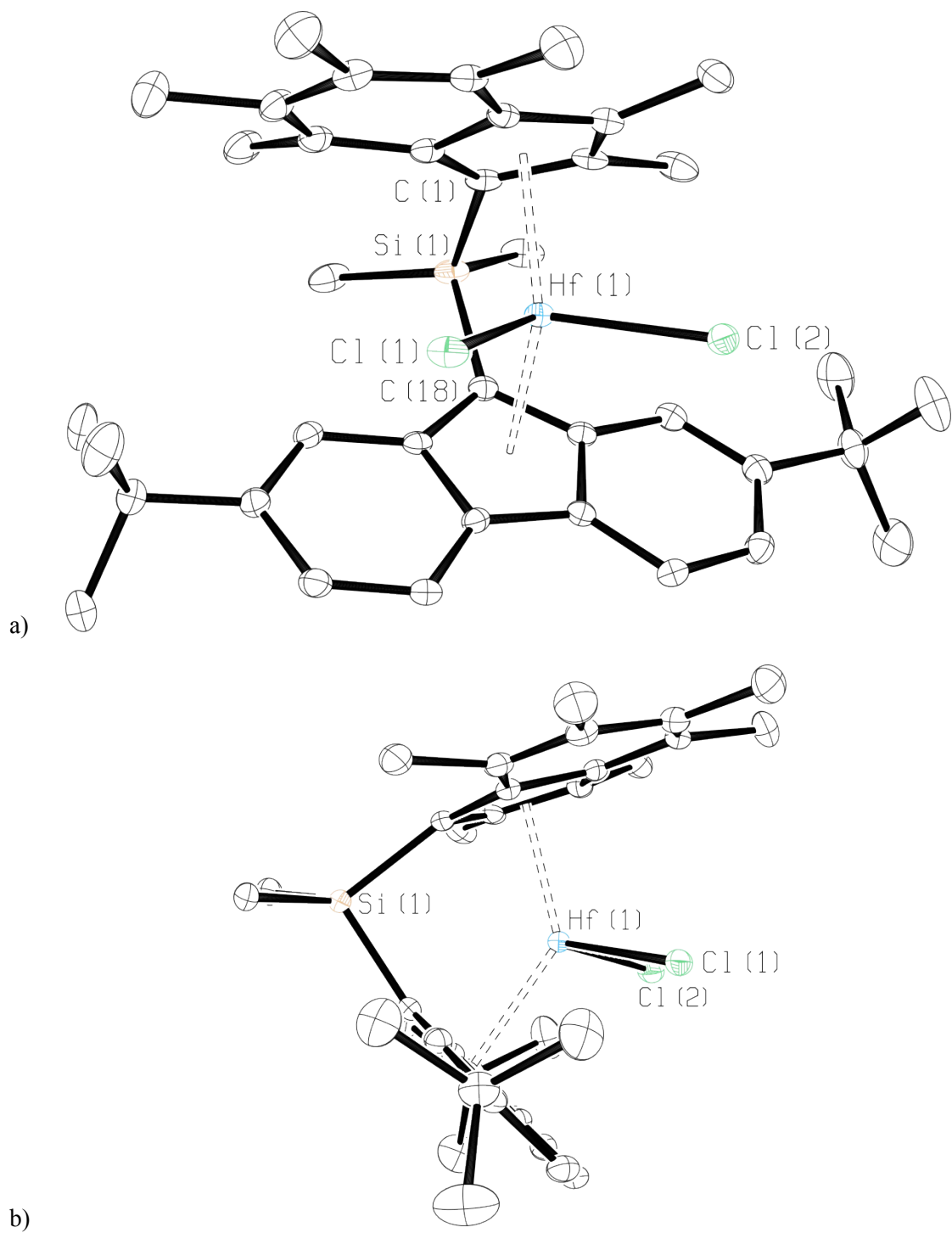


Fig. S6: Thermal displacement ellipsoid drawings (30% probability) of $^{Me_2}SB(^{t}Bu_2Flu,I^*)HfCl_2$ (**5**) a) front and b) side views. All hydrogen atoms have been omitted for clarity.

4. NMR spectroscopy

4.1 Solution NMR spectroscopy

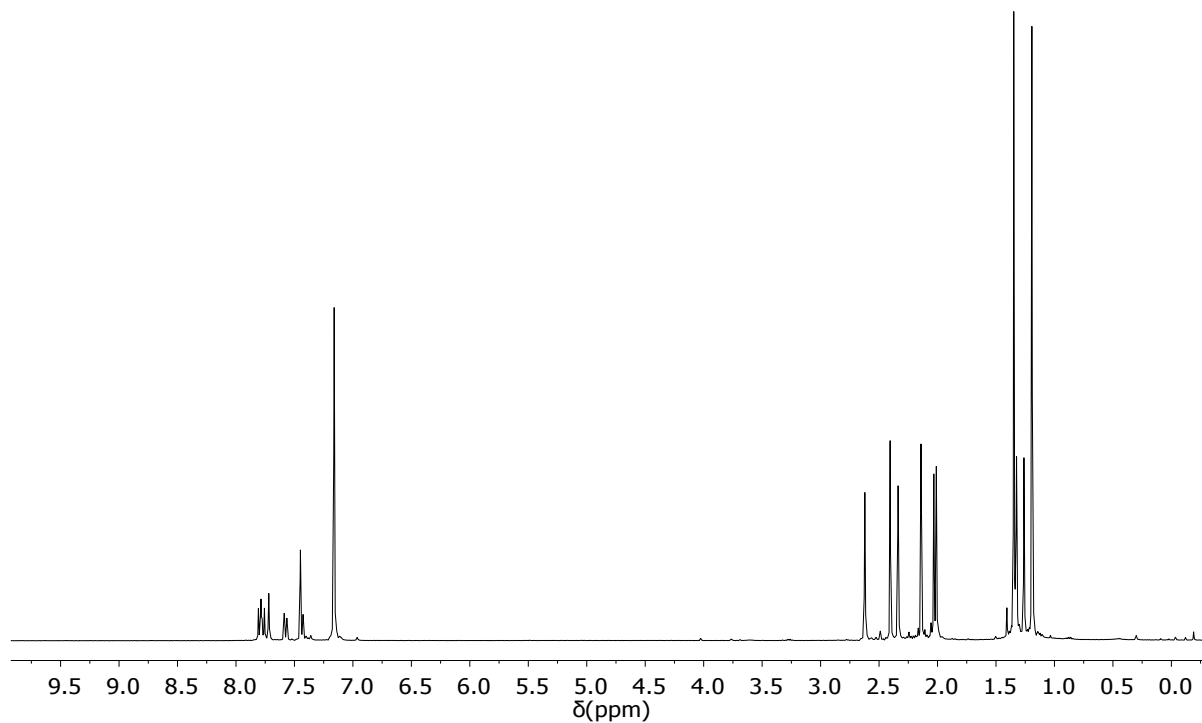


Fig. S7 ¹H NMR spectrum of ^{Me2SB(tBu2Flu,I*)ZrCl2} (**1**) (C₆D₆, 400 MHz, 298 K).

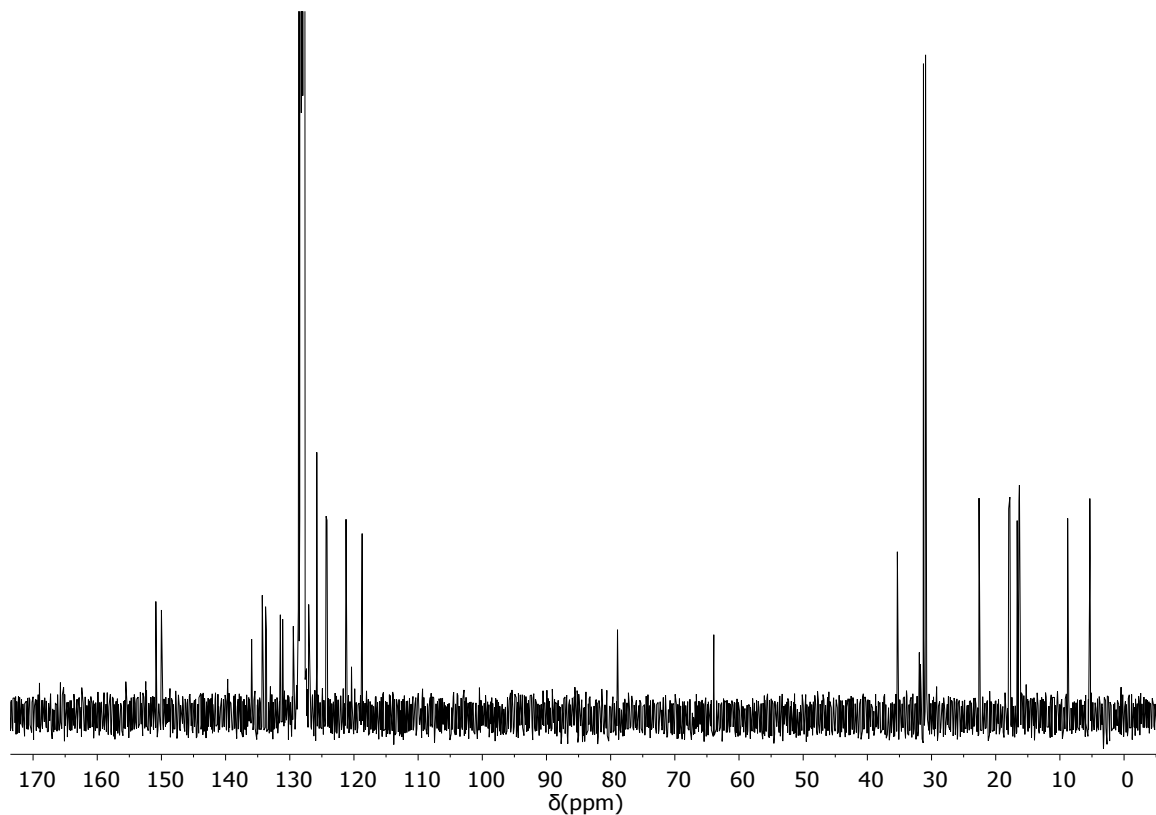


Fig. S8 ¹³C{¹H} NMR spectrum of ^{Me2SB(tBu2Flu,I*)ZrCl2} (**1**) (C₆D₆, 100 MHz, 298 K).

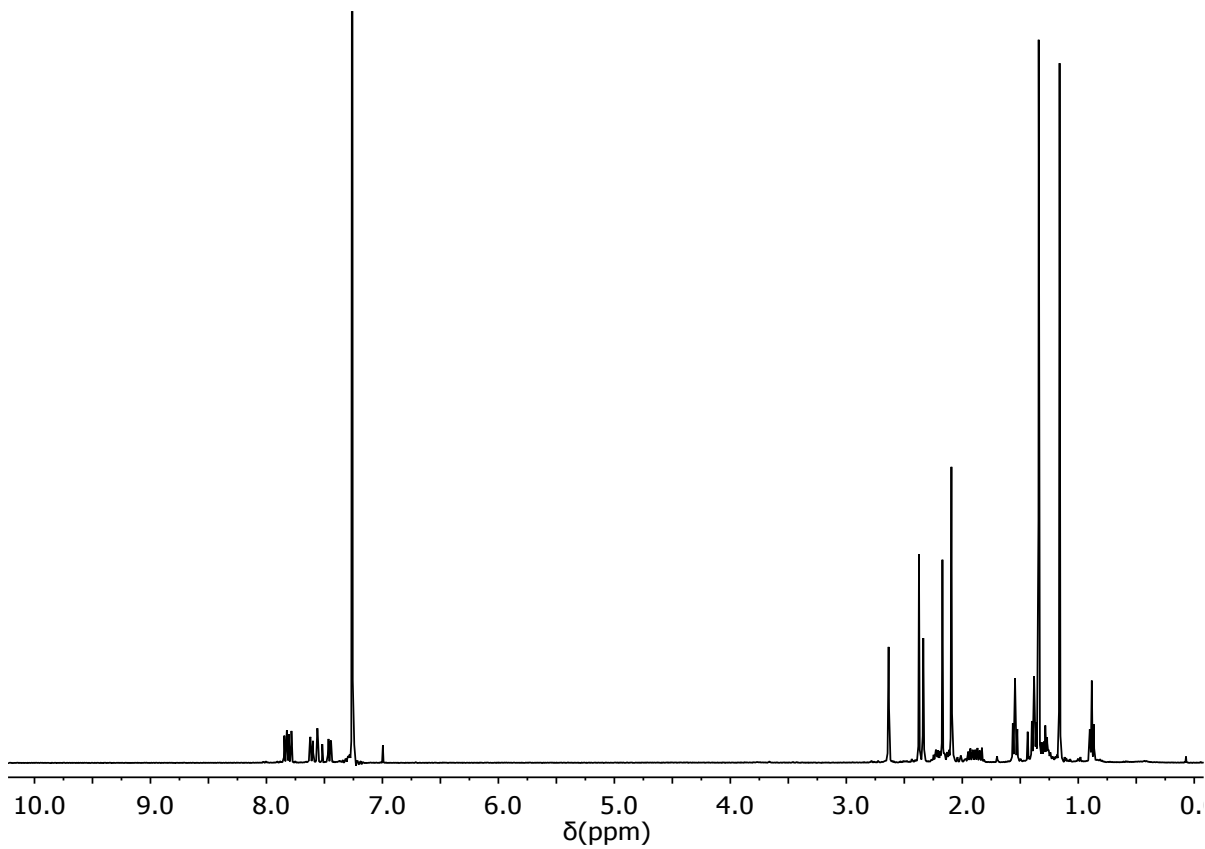


Fig. S9 ^1H NMR spectrum of $^{\text{Et}2}\text{SB}(\text{tBu}_2\text{Flu}, \text{I}^*)\text{ZrCl}_2$ (**2**) (CDCl_3 , 400 MHz, 298 K).

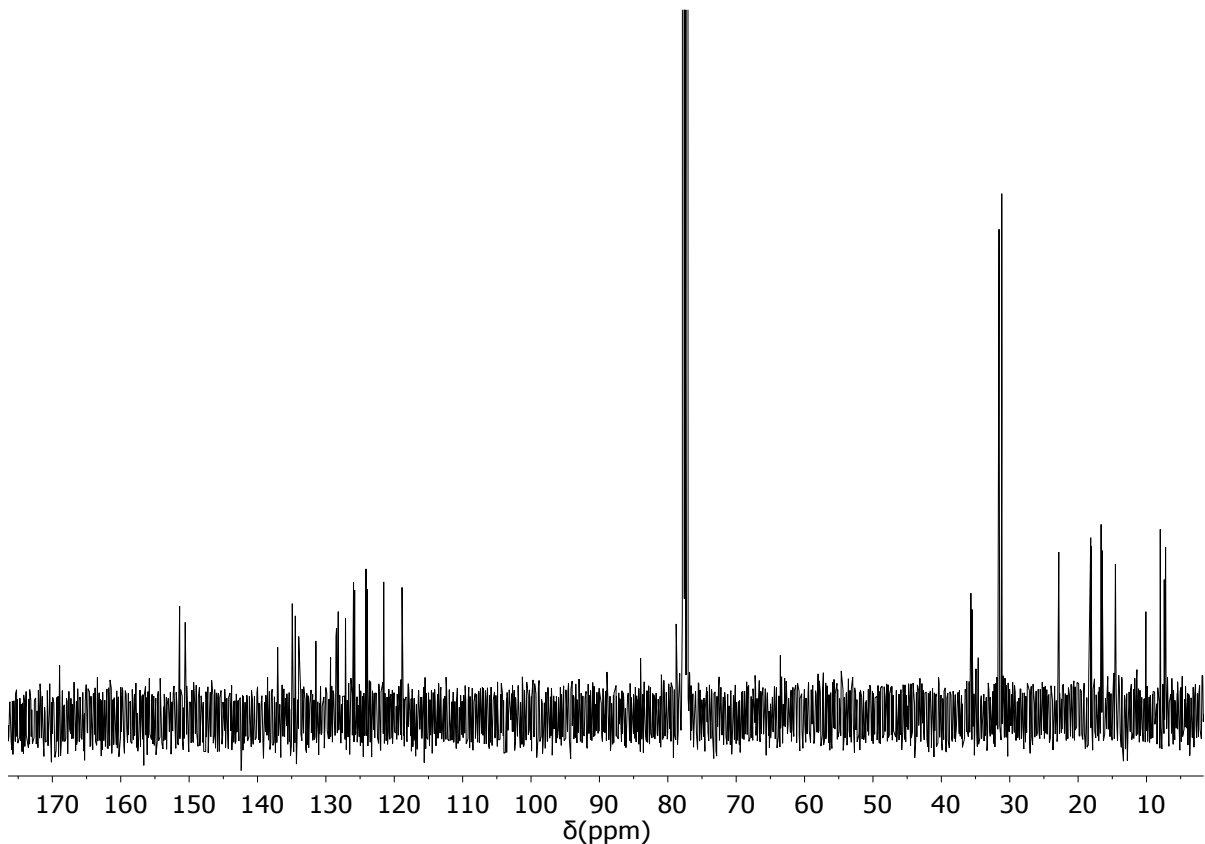


Fig. S10 $^{13}\text{C}\{^1\text{H}\}$ NMR spectrum of $^{\text{Et}2}\text{SB}(\text{tBu}_2\text{Flu}, \text{I}^*)\text{ZrCl}_2$ (**2**) (CDCl_3 , 100 MHz, 298 K).

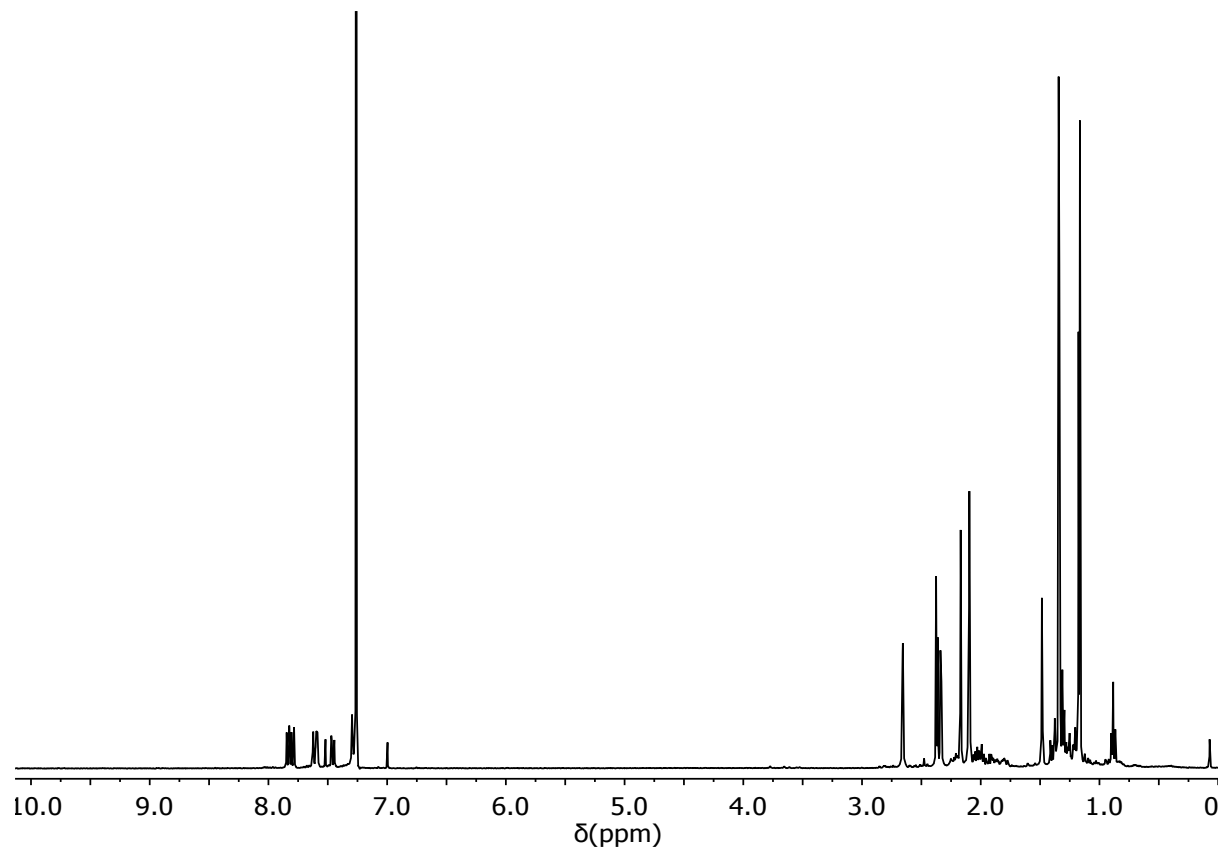


Fig. S11 ¹H NMR spectrum of ^{MePropSB(4Bu2Flu,I*)ZrCl₂} (**3**) (CDCl₃, 400 MHz, 298 K).

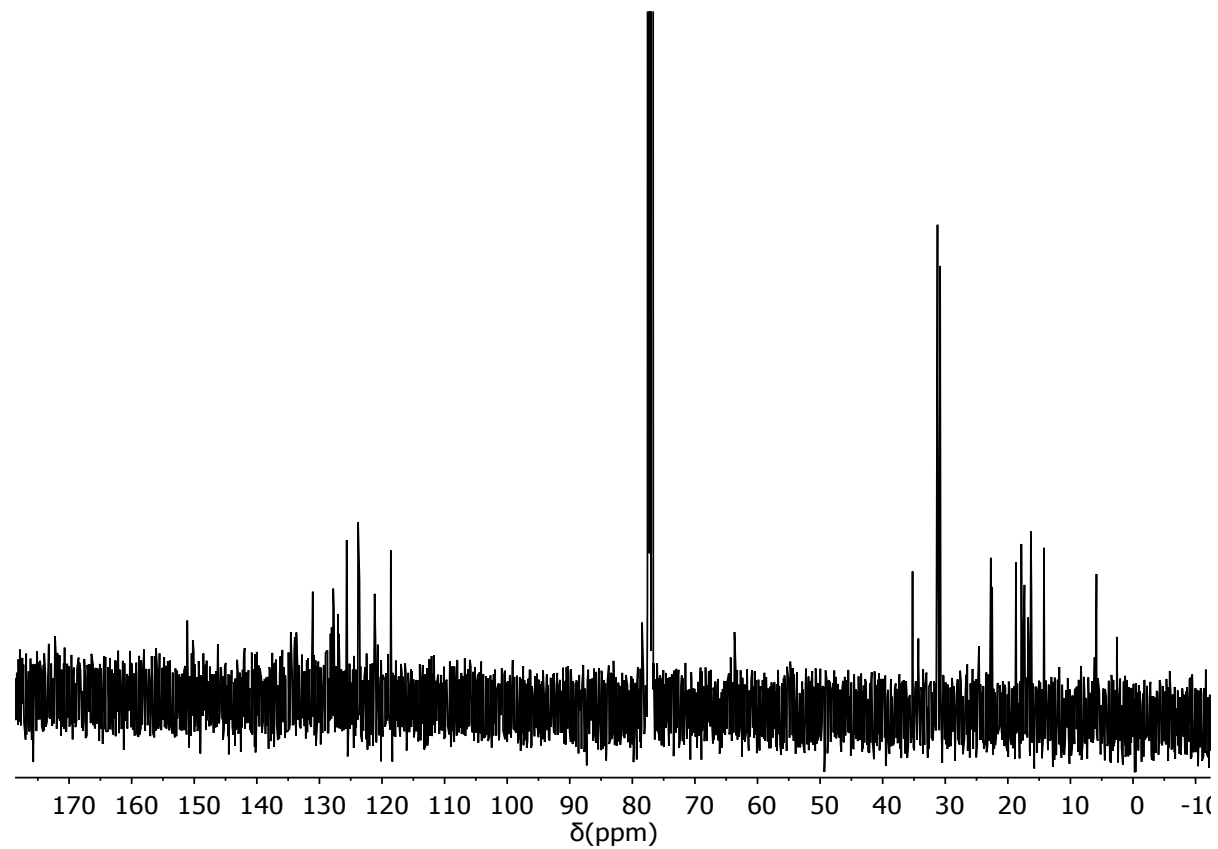


Fig. S12 ¹³C{¹H} NMR spectrum of ^{MePropSB(4Bu2Flu,I*)ZrCl₂} (**3**) (CDCl₃, 100 MHz, 298 K).

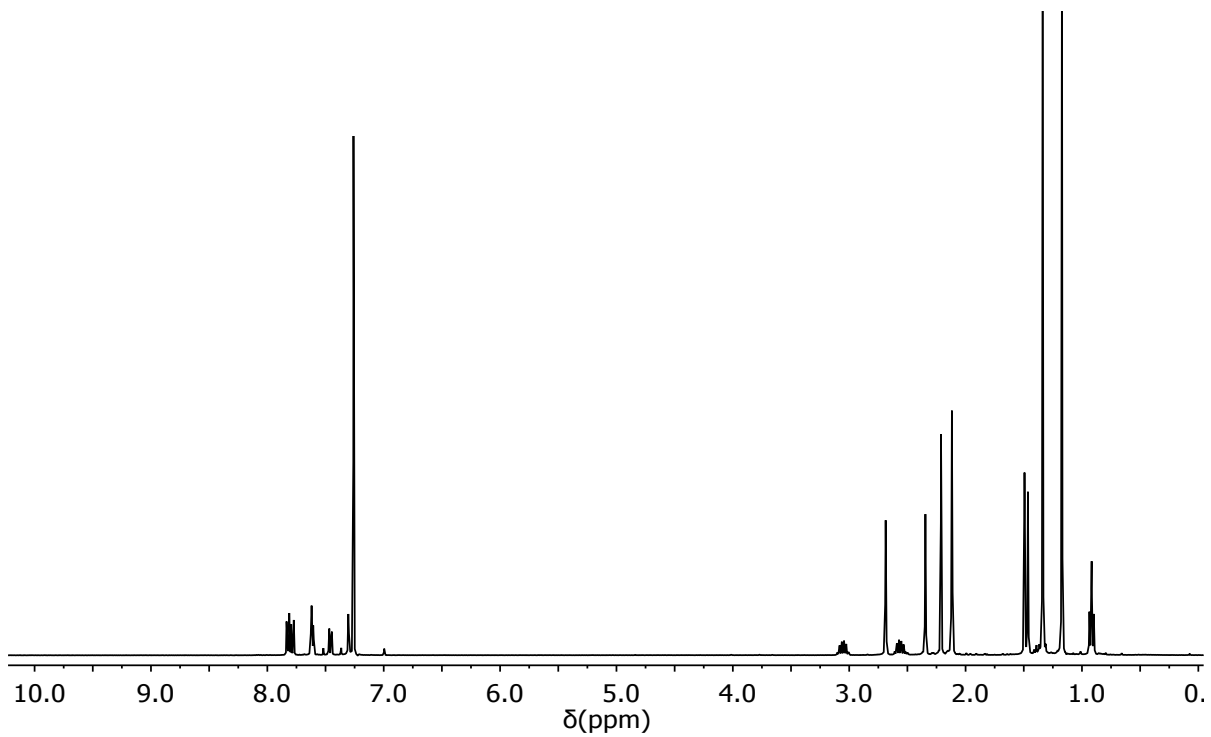


Fig. S13 ¹H NMR spectrum of ^{Me2SB(tBu2Flu,3-EtI*)ZrCl2} (**4**) (CDCl₃, 400 MHz, 298 K).

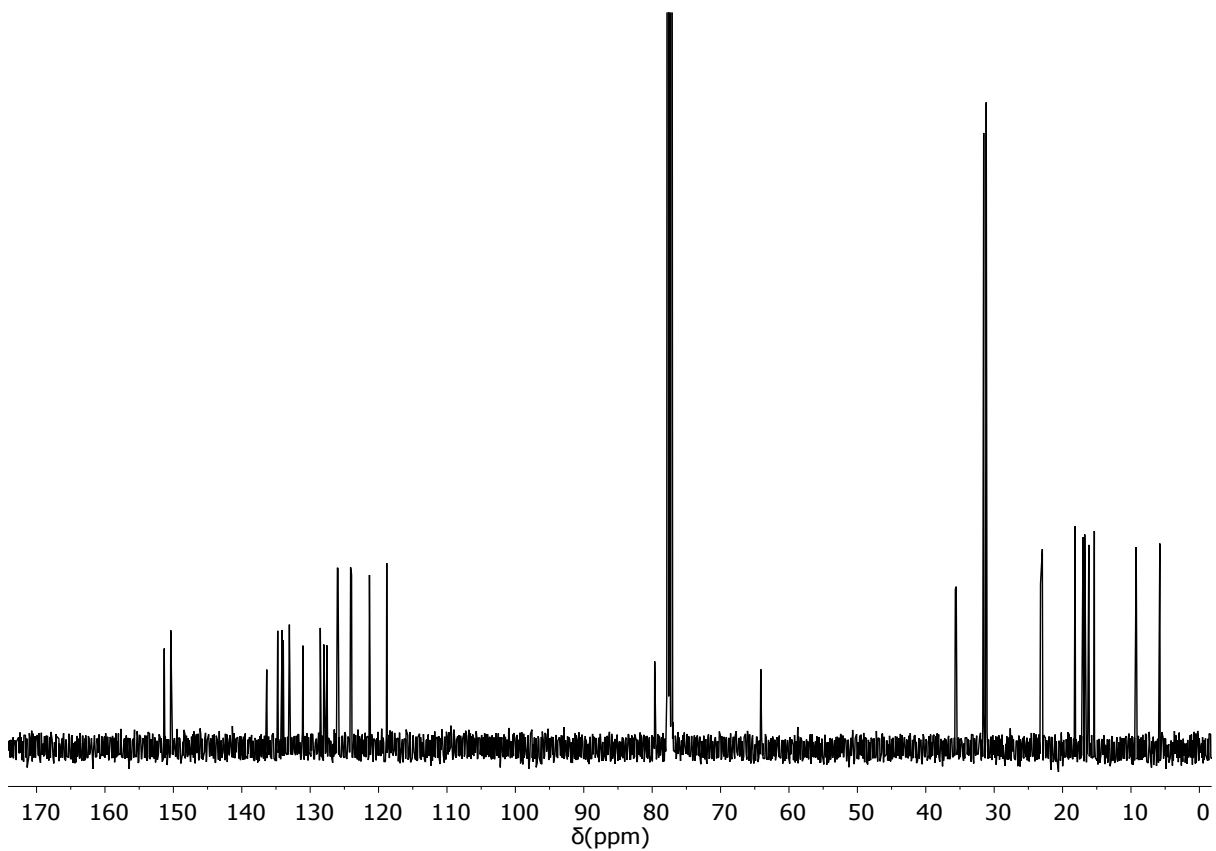


Fig. S14 ¹³C{¹H} NMR spectrum of ^{Me2SB(tBu2Flu,3-EtI*)ZrCl2} (**4**) (CDCl₃, 100 MHz, 298 K).

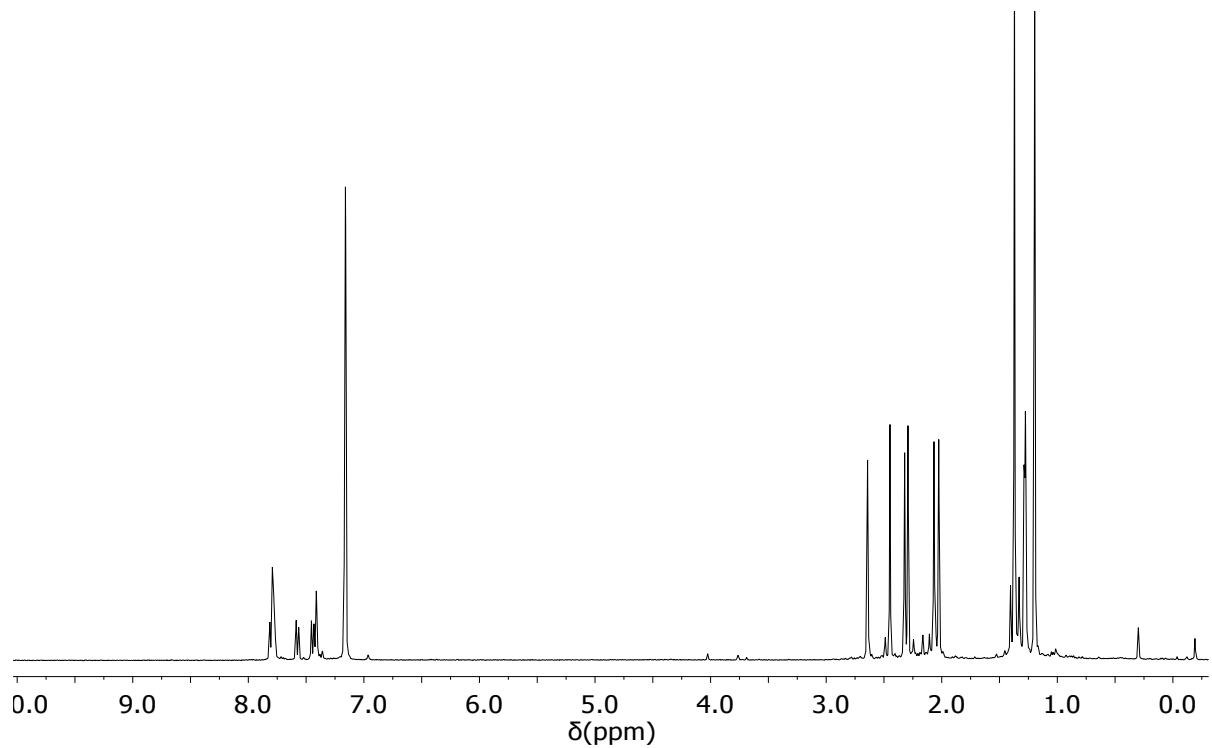


Fig. S15 ¹H NMR spectrum of ^{Me2SB(tBu2Flu,I*)HfCl2} (**5**) (C₆D₆, 400 MHz, 298 K).

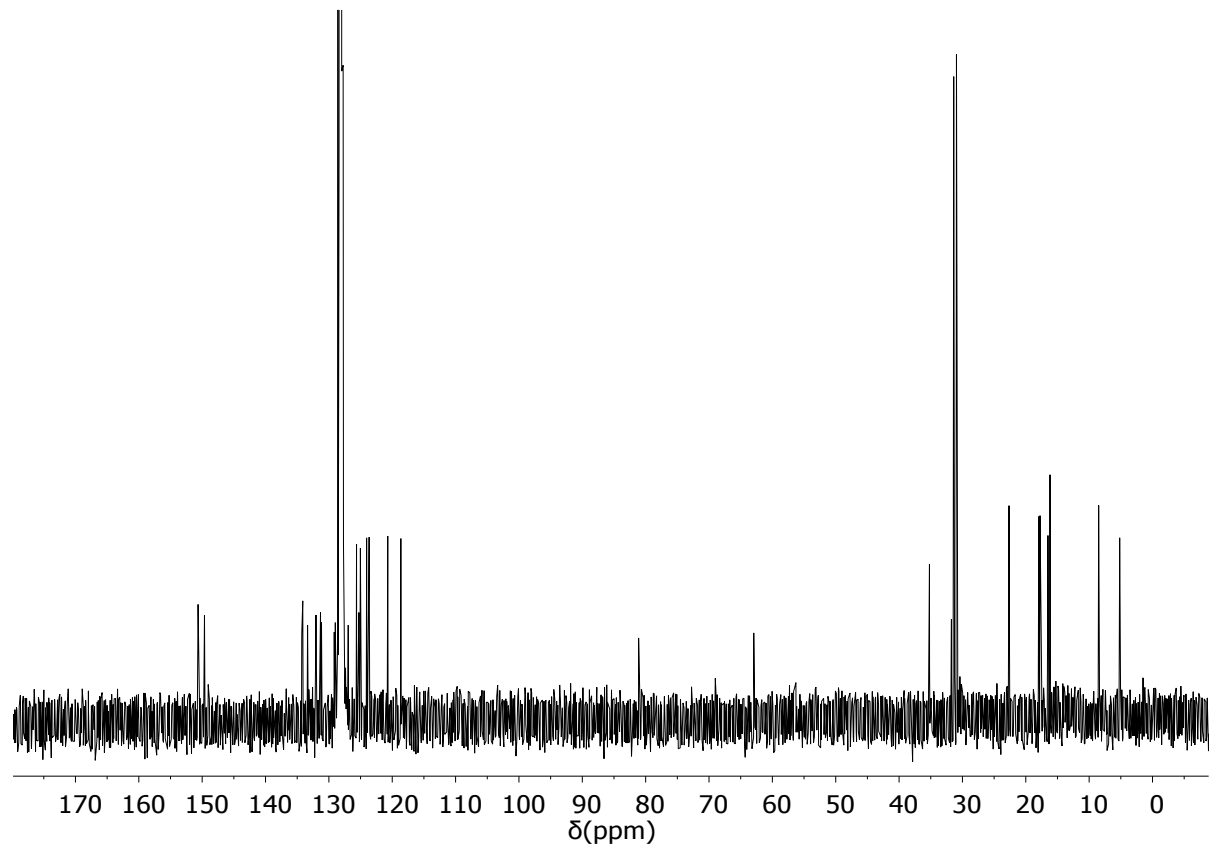


Fig. S16 ¹³C{¹H} NMR spectrum of ^{Me2SB(tBu2Flu,I*)HfCl2} (**5**) (C₆D₆, 100 MHz, 298 K).

4.2 Solid state NMR spectroscopy of solid catalysts

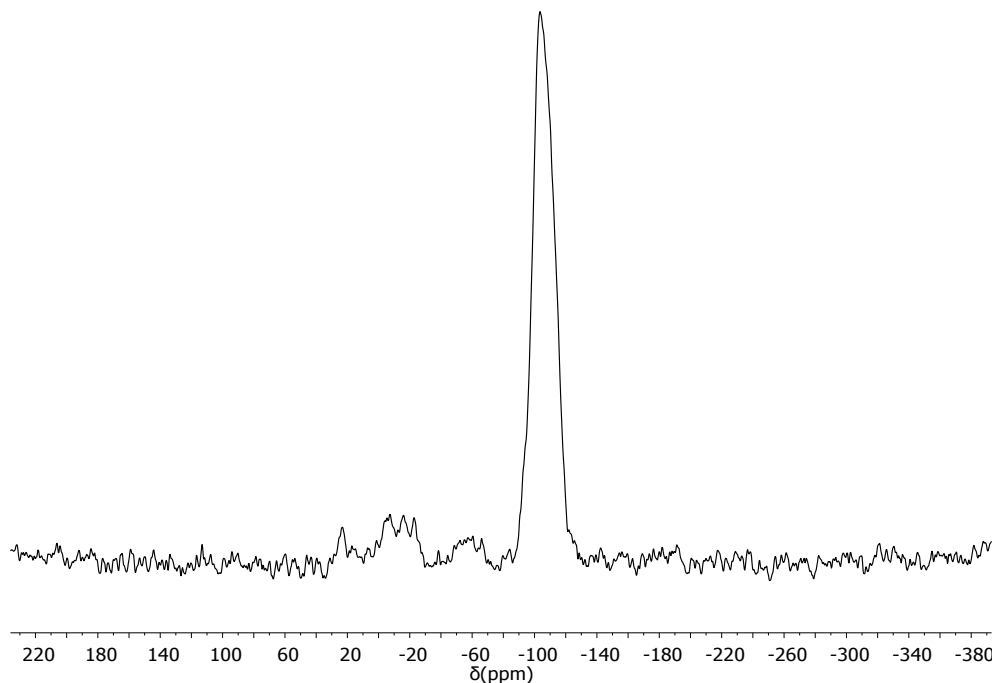


Fig. S17 ^{29}Si CPMAS (10 kHz) NMR spectrum of SSMAO- $\text{Me}_2\text{SB}(\text{tBu}_2\text{Flu}, \text{I}^*)\text{ZrCl}_2$ (**1_{SSMAO}**).

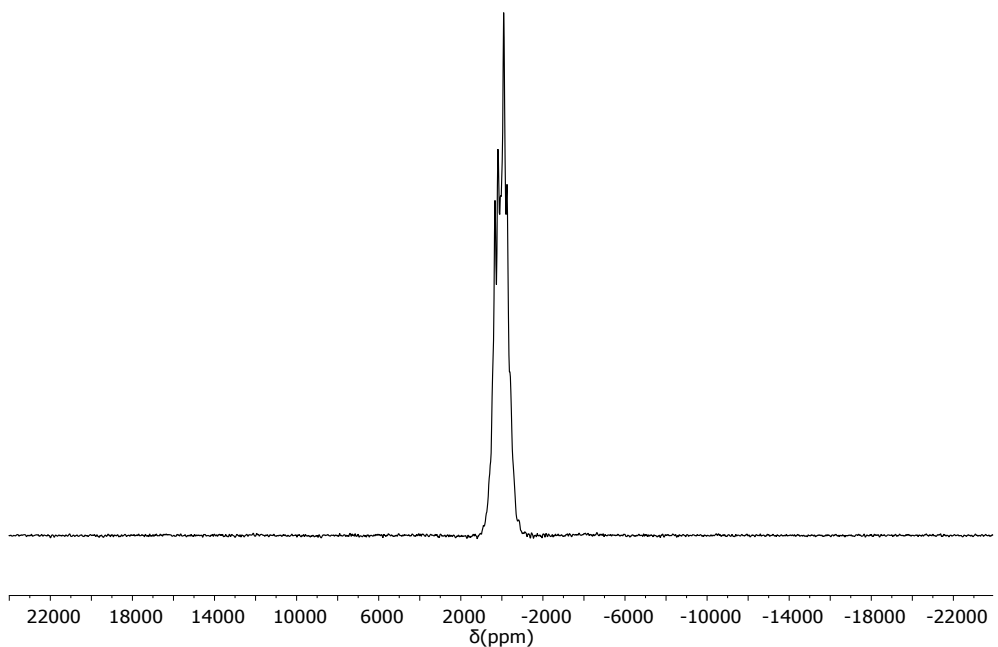


Fig. S18 ^{27}Al DPMAS hahnecho (15 kHz) NMR spectrum of SSMAO- $\text{Me}_2\text{SB}(\text{tBu}_2\text{Flu}, \text{I}^*)\text{ZrCl}_2$ (**1_{SSMAO}**).

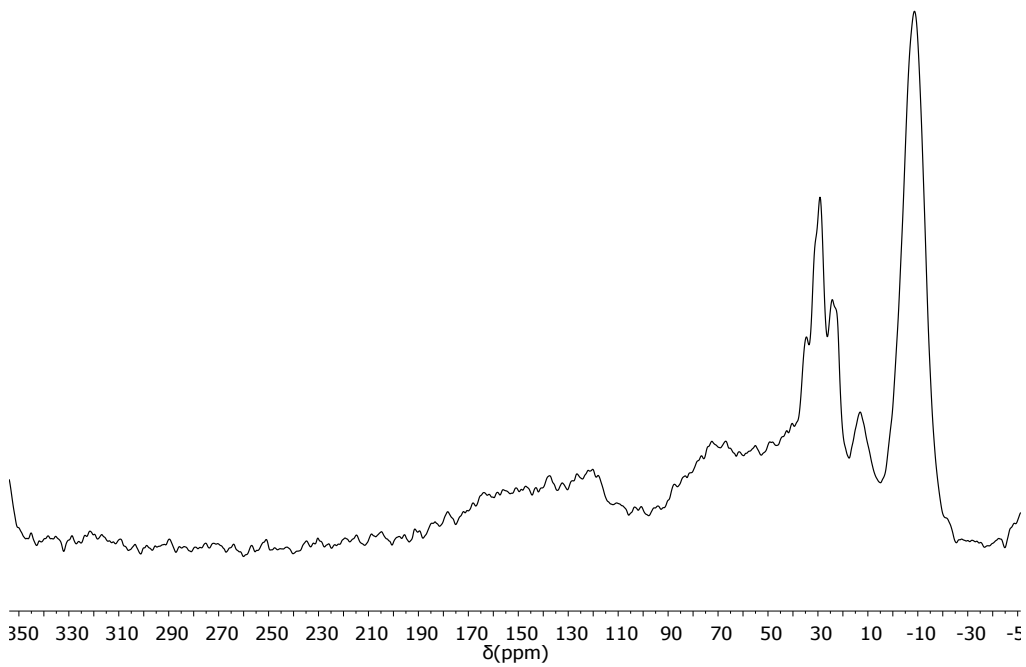


Fig. S19 ¹³C CPMAS (10 kHz) NMR spectrum of SSMAO-^{Me2SB(tBu2Flu,I*)ZrCl₂} (**1_{SSMAO}**).

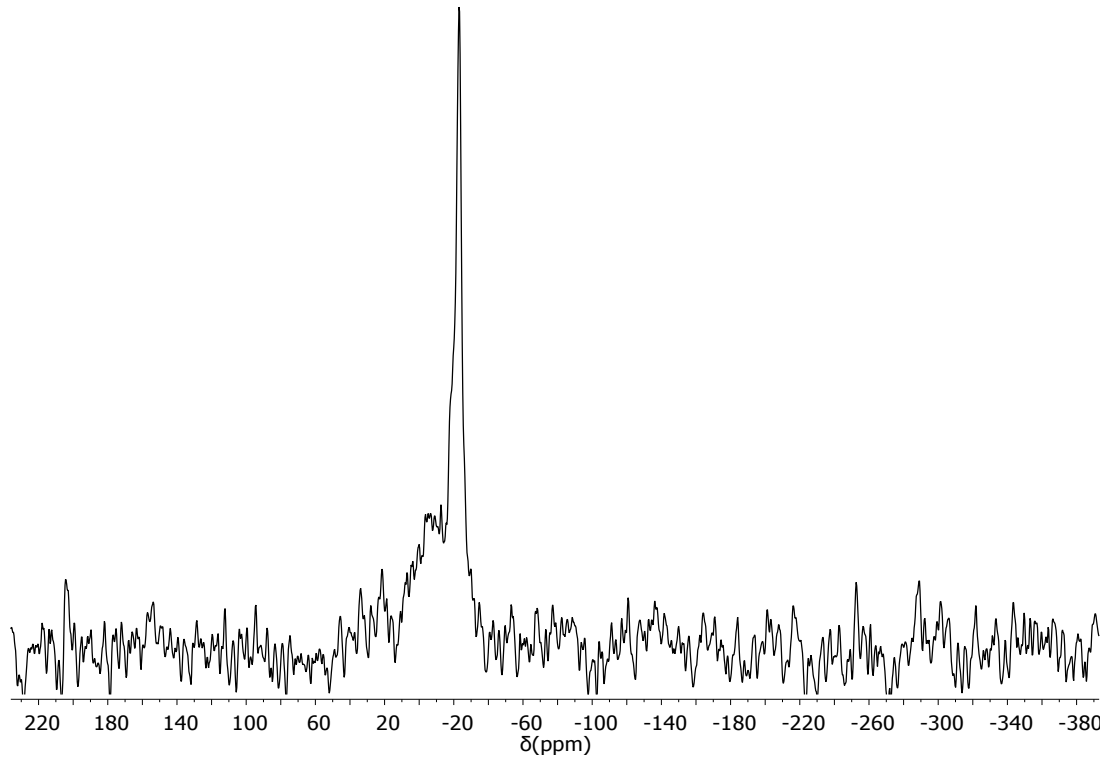


Fig. S20 ^{29}Si CPMAS (10 kHz) NMR spectrum of LDHMAO- $^{\text{Me}_2\text{SB}}(\text{tBu}_2\text{Flu}, \text{I}^*)\text{ZrCl}_2$ (**1_{LDHMAO}**).

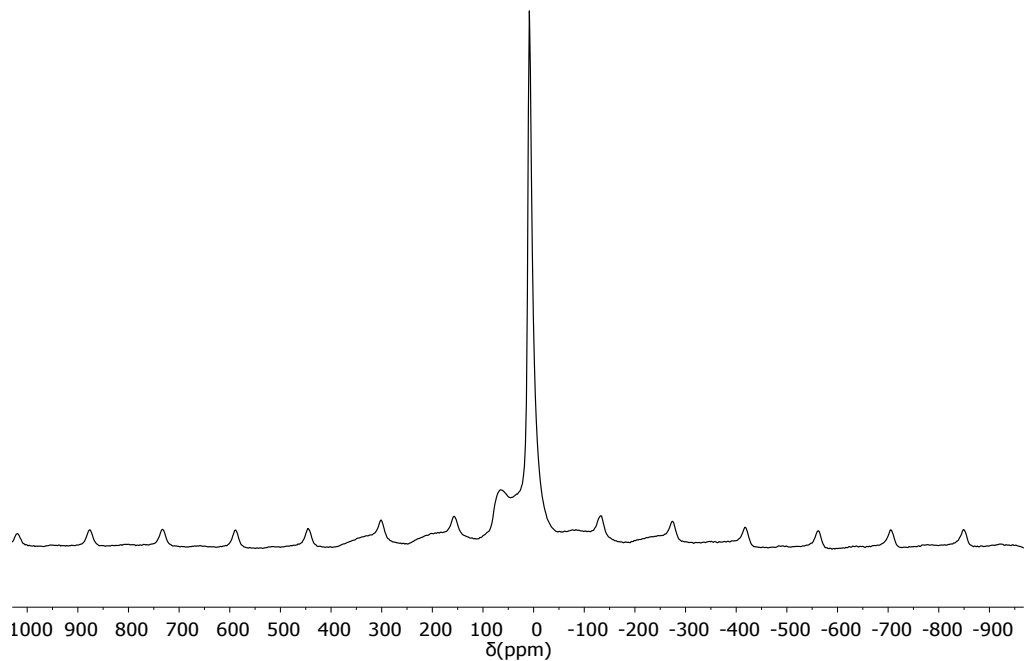


Fig. S21 ^{27}Al DPMAS (15 kHz) NMR spectrum of LDHMAO- $^{\text{Me}_2\text{SB}}(\text{tBu}_2\text{Flu}, \text{I}^*)\text{ZrCl}_2$ (**1_{LDHMAO}**).

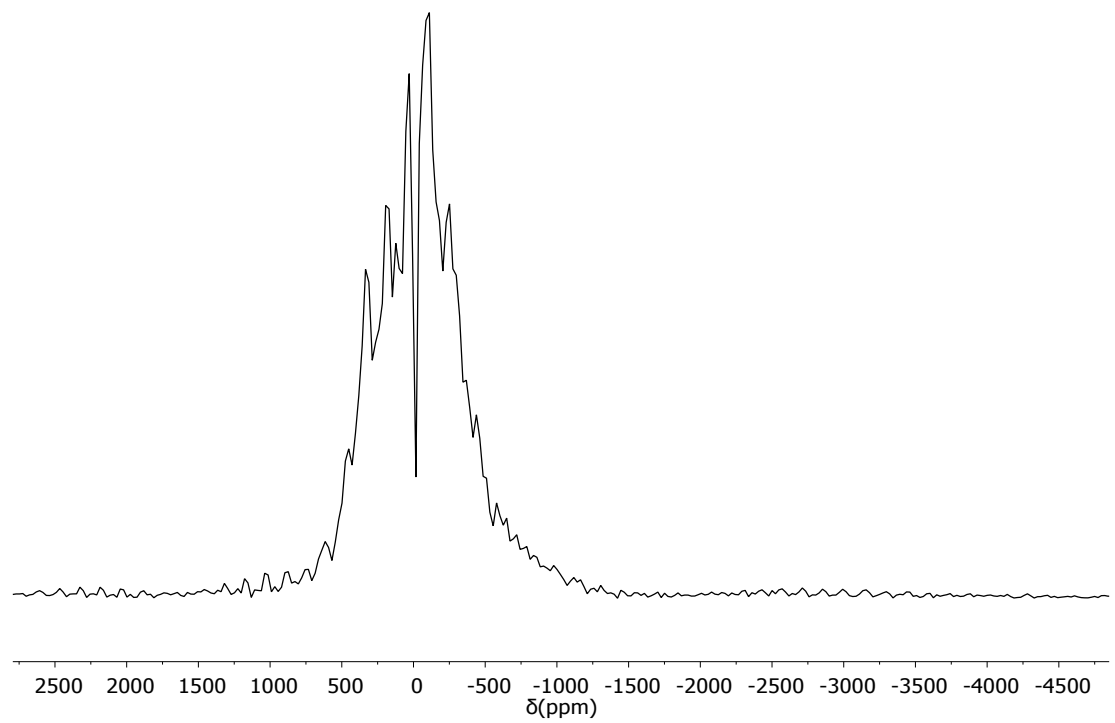


Fig. S22 ^{27}Al DPMAS (15 kHz) hahnecho NMR spectrum of LDHMAO- $\text{Me}_2\text{SB}(\text{tBu}_2\text{Flu}, \text{I}^*)\text{ZrCl}_2$ (**1_{LDHMAO}**).

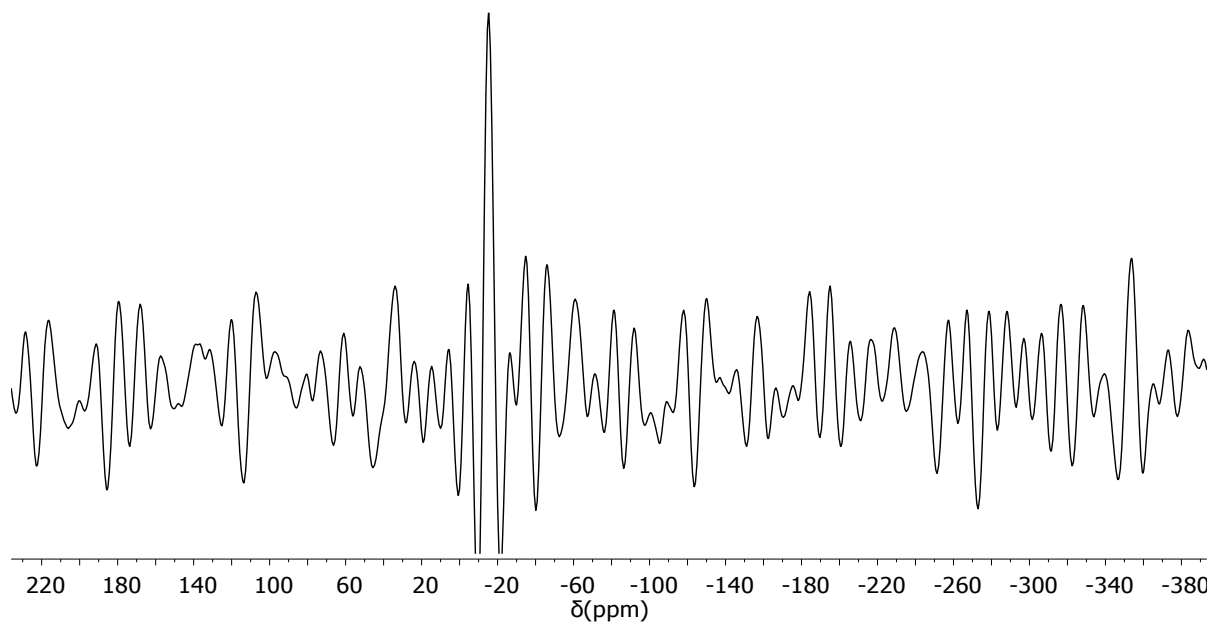


Fig. S23 ^{29}Si CPMAS (10 kHz, 200 MHz spectrometer) NMR spectrum of sMAO- $\text{Me}_2\text{SB}(\text{tBu}_2\text{Flu}, \text{I}^*)\text{ZrCl}_2$ (**1_{sMAO}**).

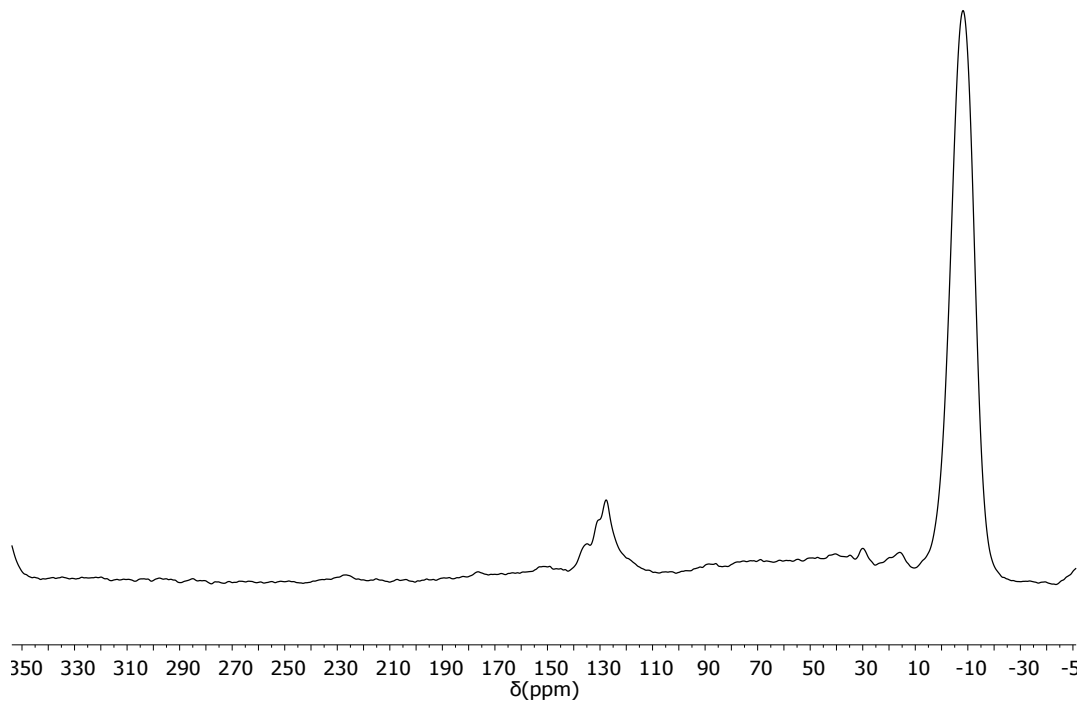


Fig. S24 ^{13}C CPMAS (10 kHz) NMR spectrum of sMAO- $\text{Me}_2\text{SB}(\text{tBu}_2\text{Flu}, \text{I}^*)\text{ZrCl}_2$ (**1_{sMAO}**).

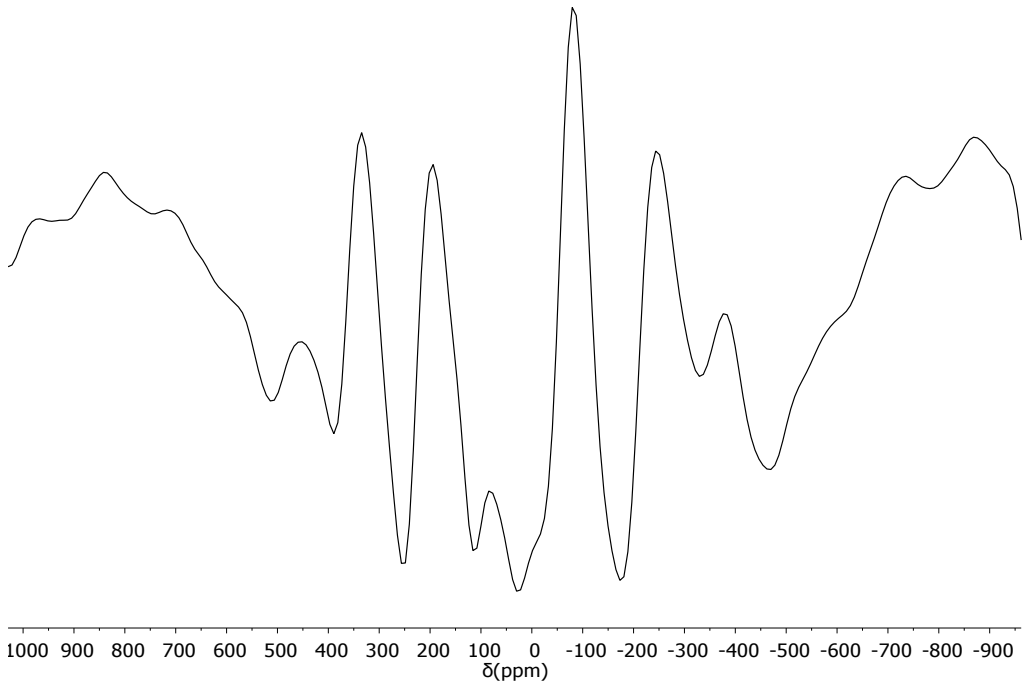


Fig. S25 ^{27}Al DPMAS (15 kHz, 200 MHz spectrometer) NMR spectrum of sMAO- $\text{Me}_2\text{SB}(\text{tBu}_2\text{Flu}, \text{I}^*)\text{ZrCl}_2$ (**1_{sMAO}**).

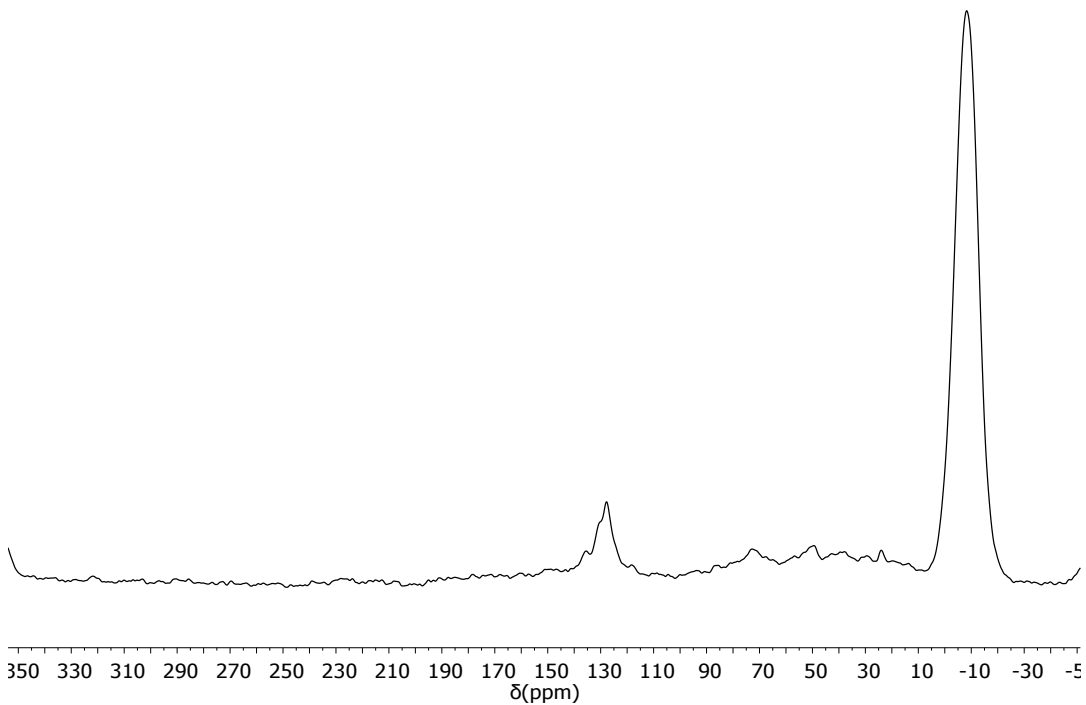


Fig. S26 ^{13}C CPMAS (10 kHz) NMR spectrum of sMAO- $\text{Et}_2\text{SB}(\text{tBu}_2\text{Flu}, \text{I}^*)\text{ZrCl}_2$ (**2_{sMAO}**).

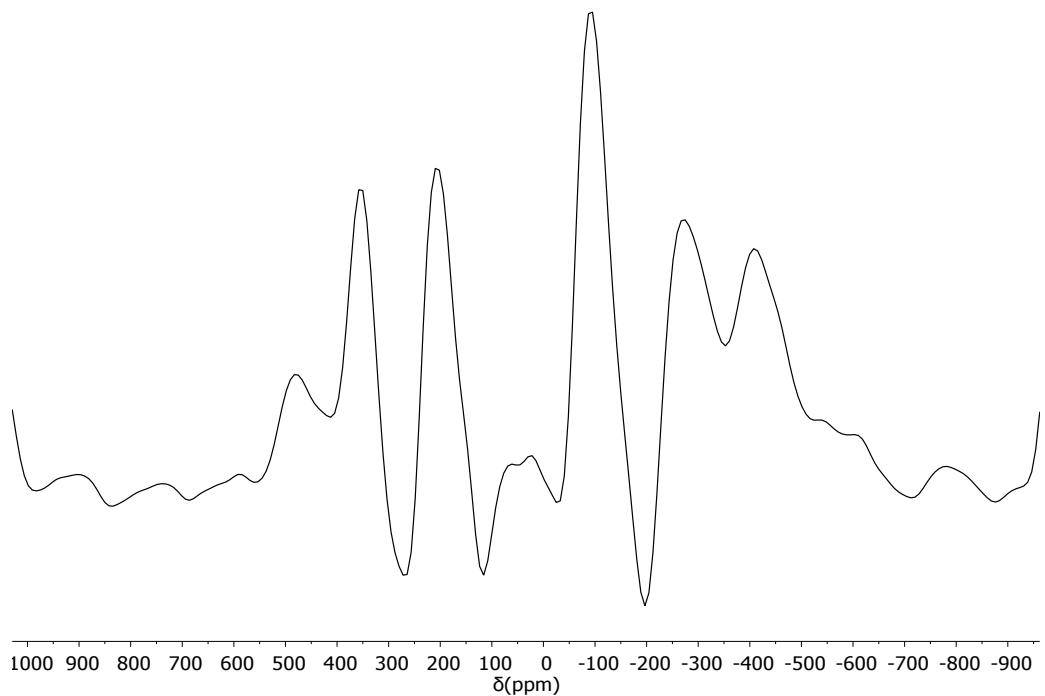


Fig. S27 ^{27}Al DPMAS (15 kHz, 200 MHz spectrometer) NMR spectrum of sMAO- $\text{Et}_2\text{SB}(\text{tBu}_2\text{Flu}, \text{I}^*)\text{ZrCl}_2$ ($\mathbf{2}_{\text{sMAO}}$).

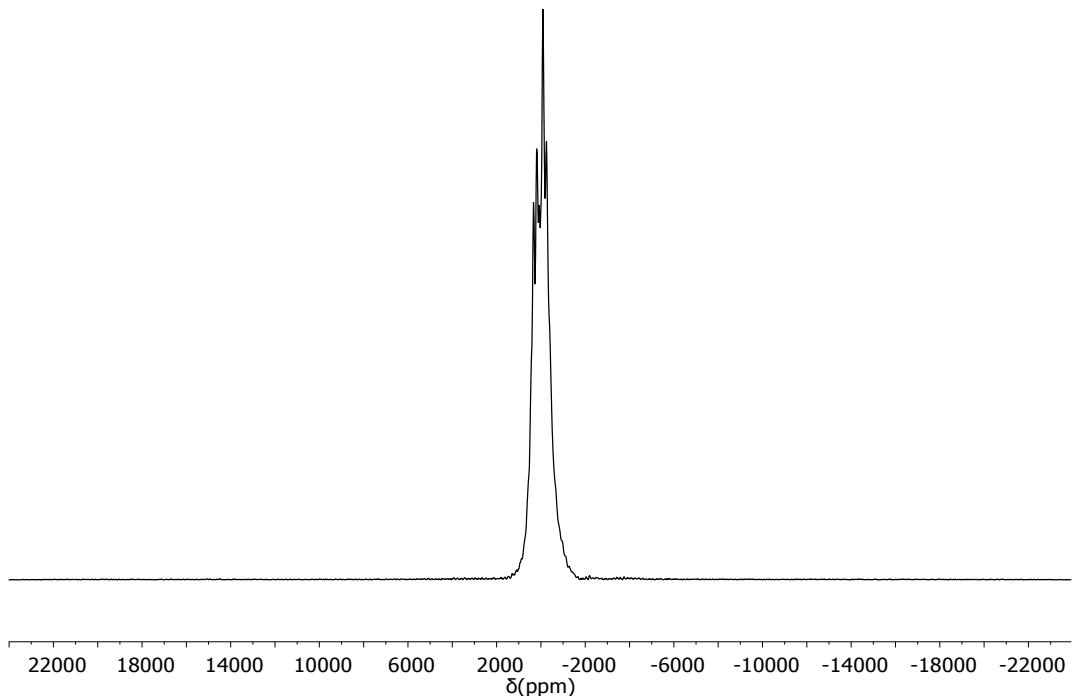


Fig. S28 ^{27}Al DPMAS (15 kHz) hahnecho NMR spectrum of sMAO- $\text{Et}_2\text{SB}(\text{tBu}_2\text{Flu}, \text{I}^*)\text{ZrCl}_2$ ($\mathbf{2}_{\text{sMAO}}$).

5. Polymerisation study

5.1 Solution phase polymerisation

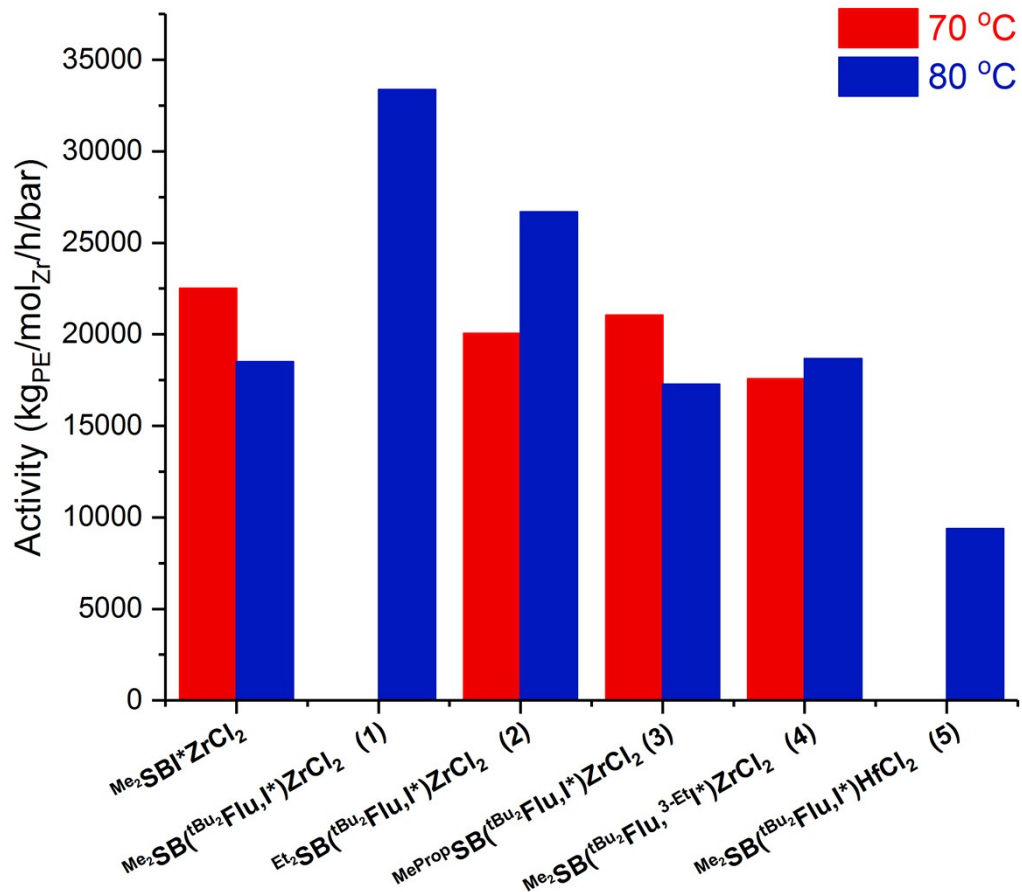


Fig. S29 Solution phase polymerisation of ethylene activities in function of complexes using $R_1R_2SB(^{t}Bu_2Flu,^{3-R}I^*)MCl_2$ and $^{Me_2}SBI^*ZrCl_2$. Polymerisation conditions: 2 bar ethylene, 50 mL hexanes, 0.5 mg complex, 5 minutes, $[MAO]_0/[Zr]_0 = 2000$.

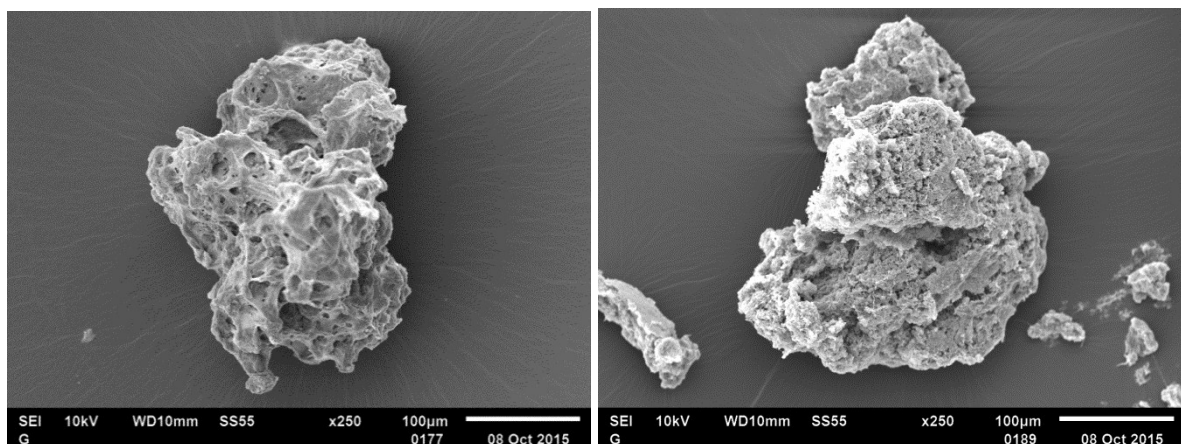


Fig. S30 SEM images of polyethylenes synthesised using $^{Me_2}SB(^{t}Bu_2Flu,I^*)ZrCl_2$ **1** (left) and $^{Et_2}SB(^{t}Bu_2Flu,I^*)ZrCl_2$ **2** (right). Polymerisation conditions: 2 bar ethylene, 50 mL hexanes, 0.5 mg complex, 5 minutes, 80 °C, $[MAO]_0/[Zr]_0 = 2000$.

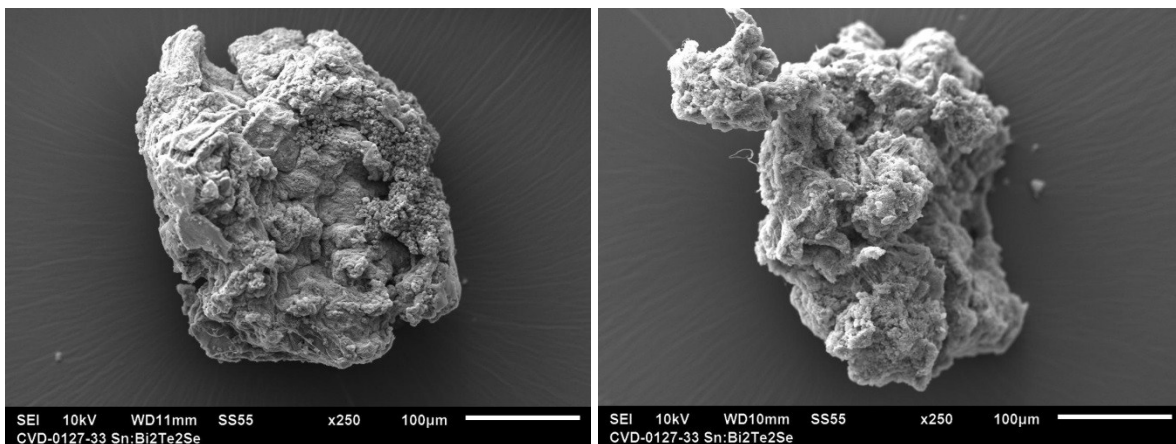


Fig. S31 SEM images of polyethylenes synthesised using $\text{MePropSB}(\text{tBu}_2\text{Flu}, \text{I}^*)\text{ZrCl}_2$ **3** (left) and $\text{Me}_2\text{SB}(\text{tBu}_2\text{Flu}, \text{Et}^3\text{I}^*)\text{ZrCl}_2$ **4** (right). Polymerisation conditions: 2 bar ethylene, 50 mL hexanes, 0.5 mg complex, 5 minutes, 80 °C, $[\text{MAO}]_0/[\text{Zr}]_0 = 2000$.

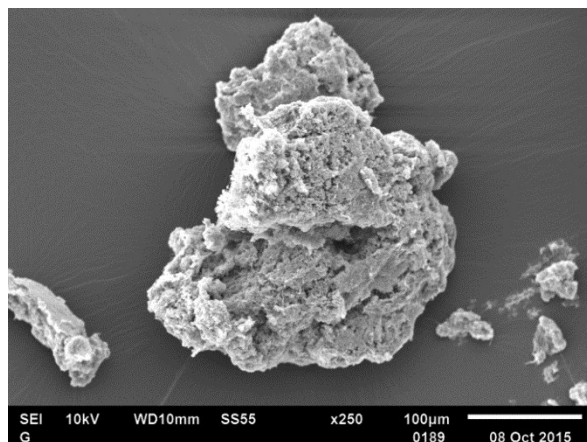


Fig. S32 SEM images of polyethylene synthesised using $\text{Me}_2\text{SB}(\text{tBu}_2\text{Flu}, \text{I}^*)\text{HfCl}_2$ **5**. Polymerisation conditions: 2 bar ethylene, 50 mL hexanes, 0.5 mg complex, 5 minutes, 80 °C, $[\text{MAO}]_0/[\text{Zr}]_0 = 2000$.

Table S4. Slurry phase polymerisation of ethylene using MAO modified silica supported catalysts.

Complex	T (°C)	Time (minutes)	Activity (kg _{PE} /mol _{Zr} /h/bar)
SBI*ZrCl₂	70	5	22500
SBI*ZrCl₂	80	5	18500
1	80	5	33360
2	70	5	20044
2	80	5	26681
3	70	5	21041
3	80	5	17267
4	70	5	17570
4	80	5	18676
5	80	5	9374

Polymerisation conditions: 2 bar ethylene, 50 mL hexanes, 0.5 mg complex, $[\text{MAO}]_0/[\text{Zr}]_0 = 2000$.

5.2 SSMAO based slurry phase polymerisation

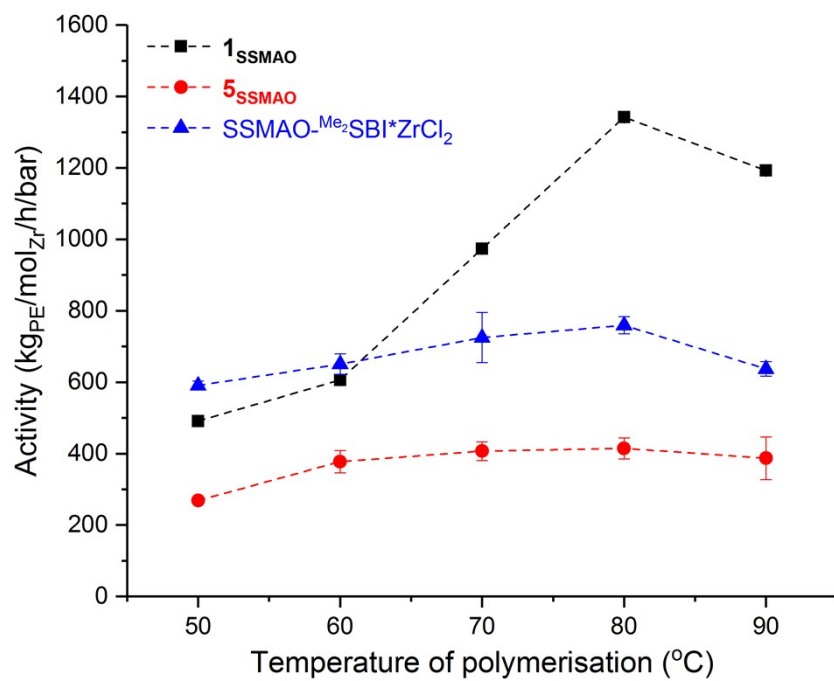


Fig. S33 Slurry phase polymerisation of ethylene activities in function of temperature using SSMAO-^{Me₂}SB(^tBu₂Flu,I*)ZrCl₂ **1_{SSMAO}** (black square), SSMAO-^{Me₂}SB(^tBu₂Flu,I*)HfCl₂ **5_{SSMAO}** (red circle) and SSMAO-^{Me₂}SBI*ZrCl₂ (blue triangle). Polymerisation conditions: 2 bar ethylene, 50 mL hexanes, 10 mg pre-catalyst, 150 mg TIBA, 30 minutes.

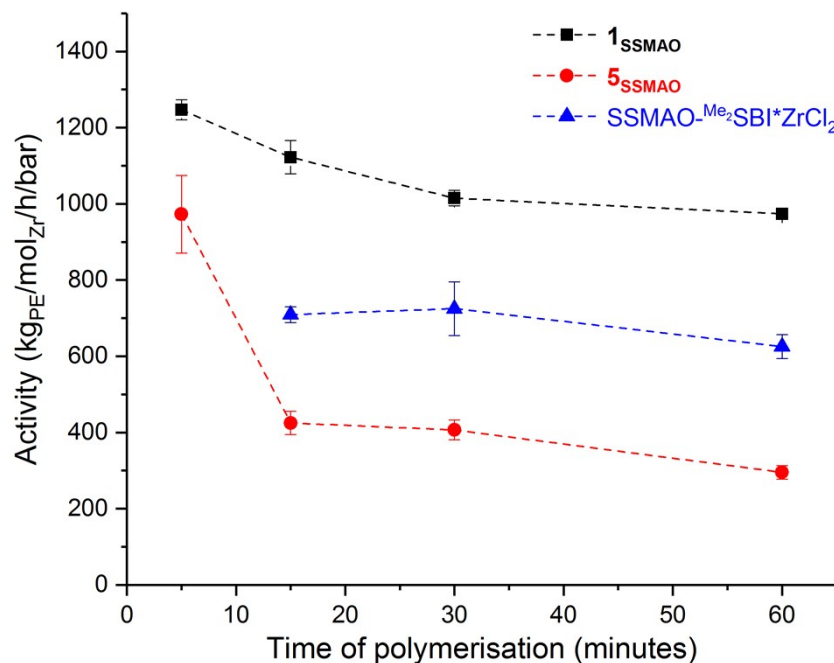


Fig. S34 Slurry phase polymerisation of ethylene activities in function of time using SSMAO-^{Me₂}SB(^tBu₂Flu,I*)ZrCl₂ **1_{SSMAO}** (black square), SSMAO-^{Me₂}SB(^tBu₂Flu,I*)HfCl₂ **5_{SSMAO}** (red circle) and SSMAO-^{Me₂}SBI*ZrCl₂ (blue triangle). Polymerisation conditions: 2 bar ethylene, 50 mL hexanes, 10 mg pre-catalyst, 150 mg TIBA, 70 °C.

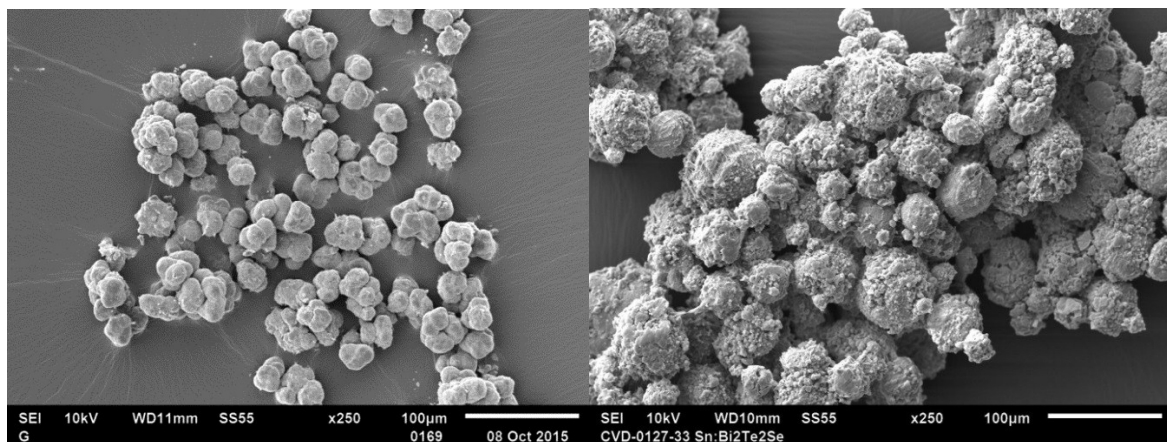


Fig. S35 SEM images of polyethylenes synthesised using $\text{SSMAO-}^{\text{Me}_2\text{SB}(^{\text{t}}\text{Bu}_2\text{Flu}, \text{I}^*)}\text{ZrCl}_2$ **1_{SSMAO}** (left) and $\text{SSMAO-}^{\text{Me}_2\text{SB}(^{\text{t}}\text{Bu}_2\text{Flu}, \text{I}^*)}\text{HfCl}_2$ **5_{SSMAO}** (right). Polymerisation conditions: 2 bar ethylene, 50 mL hexanes, 10 mg pre-catalyst, 150 mg TIBA, 30 minutes.

Table S5. Slurry phase polymerisation of ethylene using MAO modified silica supported catalysts

Complex	T (°C)	Time (minutes)	Activity (kg _{PE} /mol _{Zr} /h/bar)	M_w (kg/mol)	M_w/M_n
1_{SSMAO}	50	30	492 ± 5	1018	2.7
	60	30	606 ± 2	834	2.6
	70	30	1015 ± 20	698	2.6
	80	30	1342 ± 9	579	2.7
	90	30	1192 ± 15	480	2.7
	70	5	1247 ± 27	-	--
	70	15	1122 ± 44	-	-
	70	60	974 ± 4	-	-
5_{SSMAO}	50	30	269 ± 8	-	-
	60	30	378 ± 31	-	-
	70	30	407 ± 26	-	-
	80	30	414 ± 29	-	-
	90	30	387 ± 60	-	-
	70	5	972 ± 101	-	-
	70	15	425 ± 30	-	-
	70	60	296 ± 18	-	-
SSMAO-$^{\text{Me}_2\text{SBI}^*}\text{ZrCl}_2$	50	30	591 ± 12	-	-
	60	30	651 ± 28	-	-
	70	30	725 ± 70	-	-
	80	30	759 ± 24	-	-
	90	30	637 ± 20	-	-
	70	15	709 ± 21	-	-
	70	60	625 ± 31	-	-

Polymerisation conditions: 2 bar ethylene, 50 mL hexanes, 10 mg pre-catalyst, 150 mg TIBA.

5.3 LDHMAO based slurry phase polymerisation

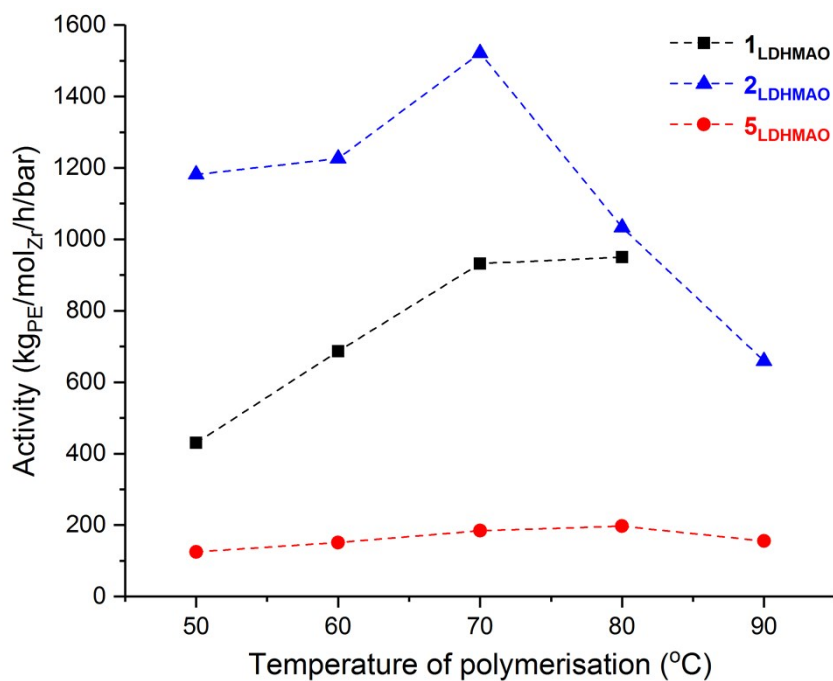


Fig. S36 Slurry phase polymerisation of ethylene activities in function of temperature using LDHMAO- $\text{Me}_2\text{SB}(\text{^tBu}_2\text{Flu}, \text{I}^*)\text{ZrCl}_2$ **1_{LDHMAO}** (black square), LDHMAO- $\text{Et}_2\text{SB}(\text{^tBu}_2\text{Flu}, \text{I}^*)\text{ZrCl}_2$ **2_{LDHMAO}** (blue triangle) and LDHMAO- $\text{Me}_2\text{SB}(\text{^tBu}_2\text{Flu}, \text{I}^*)\text{HfCl}_2$ **5_{LDHMAO}** (red circle). Polymerisation conditions: 2 bar ethylene, 50 mL hexanes, 10 mg pre-catalyst, 150 mg TIBA, 30 minutes.

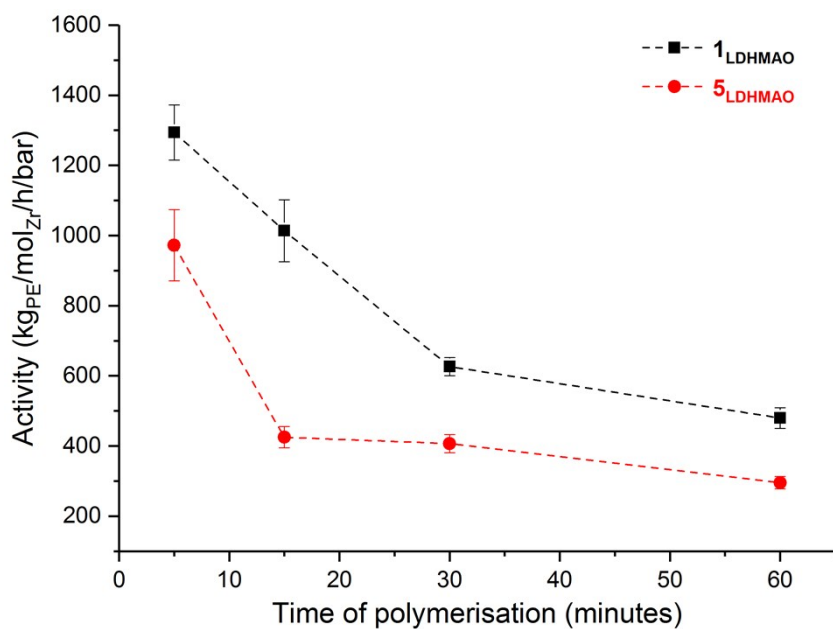


Fig. S37 Slurry phase polymerisation of ethylene activities in function of temperature using LDHMAO- $\text{Me}_2\text{SB}(\text{^tBu}_2\text{Flu}, \text{I}^*)\text{ZrCl}_2$ **1_{LDHMAO}** (black square) and LDHMAO- $\text{Me}_2\text{SB}(\text{^tBu}_2\text{Flu}, \text{I}^*)\text{HfCl}_2$ **5_{LDHMAO}** (red circle). Polymerisation conditions: 2 bar ethylene, 50 mL hexanes, 10 mg pre-catalyst, 150 mg TIBA, 70 °C.

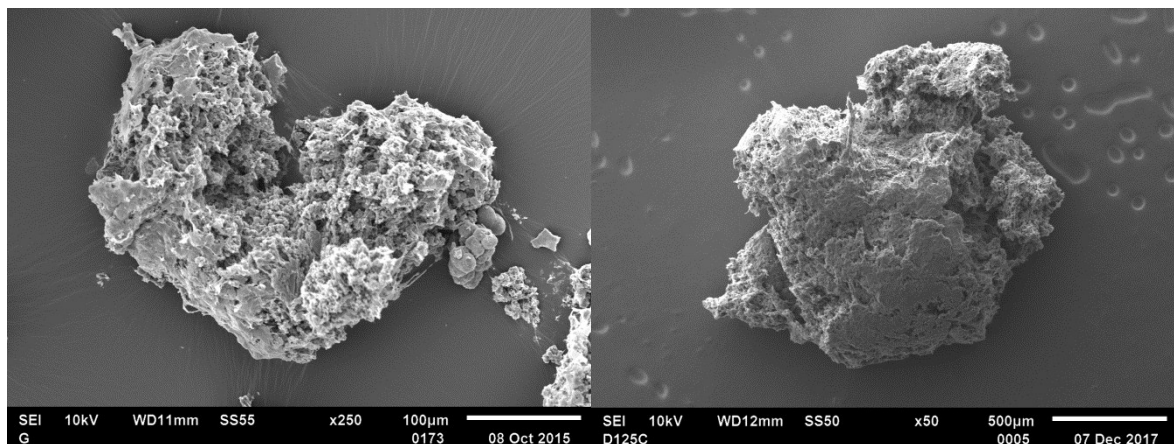


Fig. S38 SEM images of polyethylenes synthesised using LDHMAO- $\text{Me}_2\text{SB}(\text{tBu}_2\text{Flu}, \text{I}^*)\text{ZrCl}_2$ **1_{LDHMAO}** (left) and LDHMAO- $\text{Et}_2\text{SB}(\text{tBu}_2\text{Flu}, \text{I}^*)\text{ZrCl}_2$ **2_{LDHMAO}** (right). Polymerisation conditions: 2 bar ethylene, 50 mL hexanes, 10 mg pre-catalyst, 150 mg TIBA, 30 minutes.

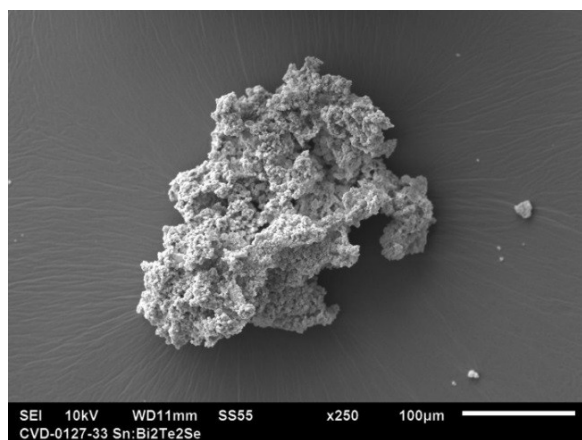


Fig. S39 SEM images of polyethylene synthesised using LDHMAO- $\text{Me}_2\text{SB}(\text{tBu}_2\text{Flu}, \text{I}^*)\text{HfCl}_2$ **5_{LDHMAO}**. Polymerisation conditions: 2 bar ethylene, 50 mL hexanes, 10 mg pre-catalyst, 150 mg TIBA, 30 minutes.

Table S6. Slurry phase polymerisation of ethylene using MAO-modified LDH supported catalysts.

Complex	T (°C)	Time (minutes)	Activity (kg _{PE} /mol _{Zr} /h/bar)	M _w (kg/mol)	M _w /M _n
1 _{LDHMAO}	50	30	430 ± 59	869	2.7
	60	30	687 ± 205	792	2.7
	70	30	932 ± 380	725	2.4
	80	30	951 ± 4	628	2.6
	90	30	1542 ± 258	519	2.4
	70	5	1294 ± 78	-	-
	70	15	1014 ± 425	-	-
	70	60	480 ± 29	-	-
2 _{LDHMAO}	50	30	1182 ± 338	890	2.5
	60	30	1226 ± 52	821	2.6
	70	30	1522 ± 344	710	2.6
	80	30	1033 ± 105	603	2.6
	90	30	659 ± 14	600	2.6
5 _{LDHMAO}	50	30	125 ± 6	1168	3.0
	60	30	151 ± 9	1112	2.9
	70	30	184 ± 26	949	2.8
	80	30	197 ± 8	844	2.7
	90	30	155 ± 8	622	2.6
	70	5	973 ± 102	-	-
	70	15	425 ± 30	-	-
	70	60	407 ± 26	-	-

Polymerisation conditions: 2 bar ethylene, 50 mL hexanes, 10 mg pre-catalyst, 150 mg TIBA.

5.4 Solid MAO based slurry phase polymerisation

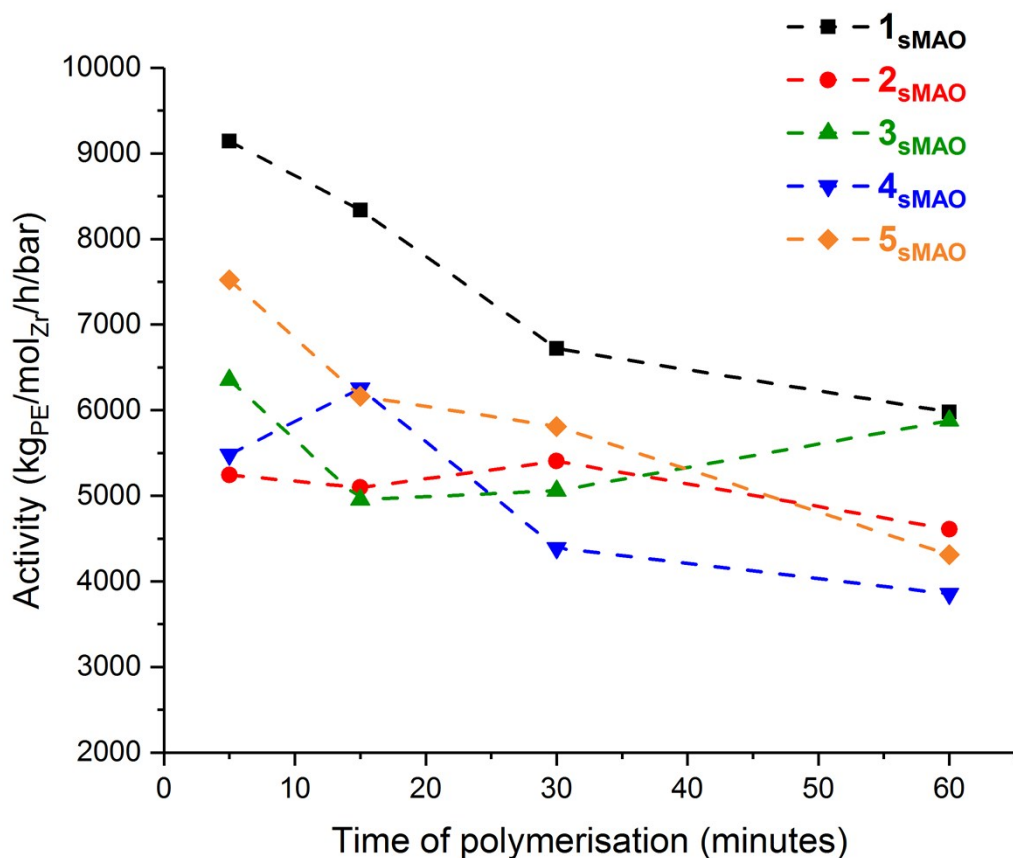


Fig. S40 Slurry phase polymerisation of ethylene activities in function of time using sMAO- $\text{Me}_2\text{SB}(\text{tBu}_2\text{Flu}, \text{I}^*)\text{ZrCl}_2$ 1_{sMAO} (black square), sMAO- $\text{Et}_2\text{SB}(\text{tBu}_2\text{Flu}, \text{I}^*)\text{ZrCl}_2$ 2_{sMAO} (red circle), sMAO- $\text{MePropSB}(\text{tBu}_2\text{Flu}, \text{I}^*)\text{ZrCl}_2$ 3_{sMAO} (green triangle), sMAO- $\text{Me}_2\text{SB}(\text{tBu}_2\text{Flu}, {}^{3-\text{Et}}\text{I}^*)\text{ZrCl}_2$ 4_{sMAO} (blue down triangle) and sMAO- $\text{Me}_2\text{SB}(\text{tBu}_2\text{Flu}, \text{I}^*)\text{HfCl}_2$ 5_{sMAO} (orange diamond). Polymerisation conditions: 2 bar ethylene, 50 mL hexanes, 10 mg pre-catalyst, 150 mg TIBA, 30 minutes.

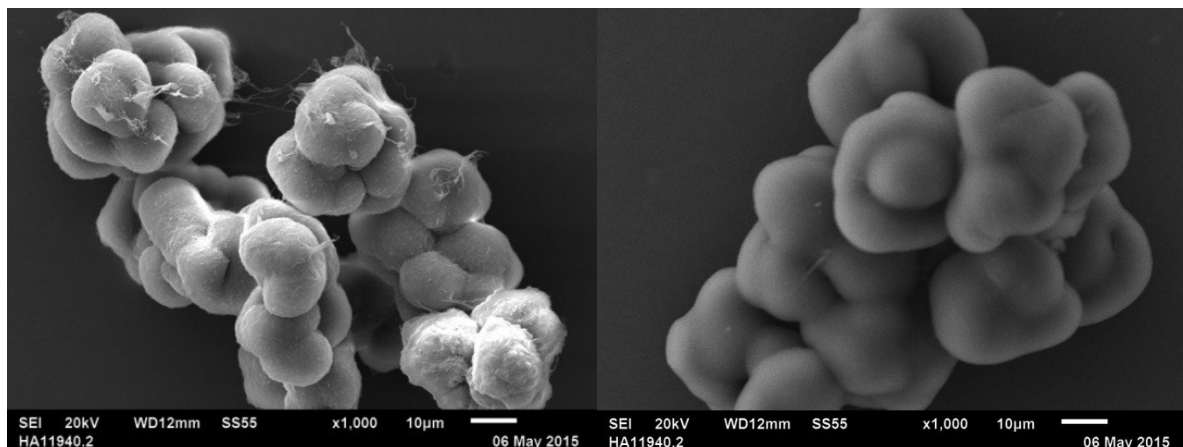


Fig. S41 SEM images of polyethylenes synthesised using sMAO- $^{Me_2}SB(^{t}Bu_2Flu,I^*)ZrCl_2$ **1_{sMAO}** (left) and sMAO-MePropSB($^{t}Bu_2Flu,I^*$)ZrCl₂ **3_{sMAO}** (right). Polymerisation conditions: 2 bar ethylene, 50 mL hexanes, 10 mg pre-catalyst, 150 mg TIBA, 30 minutes.

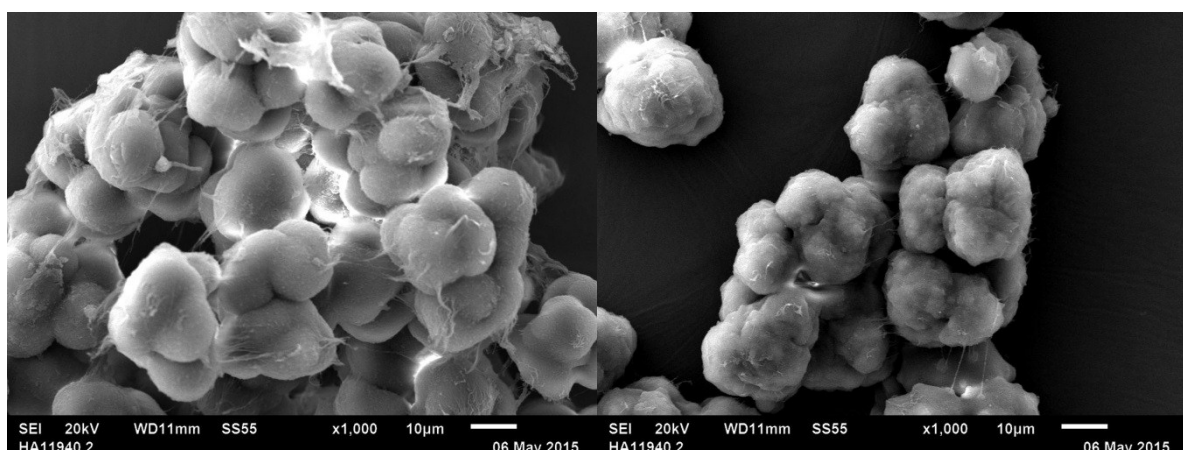


Fig. S42 SEM images of polyethylenes synthesised using sMAO- $^{Me_2}SB(^{t}Bu_2Flu,^{3-Et}I^*)ZrCl_2$ **4_{sMAO}** (left) and sMAO- $^{Me_2}SB(^{t}Bu_2Flu,I^*)HfCl_2$ **5_{sMAO}** (right). Polymerisation conditions: 2 bar ethylene, 50 mL hexanes, 10 mg pre-catalyst, 150 mg TIBA, 30 minutes.

Table S7. Slurry phase polymerisation of ethylene using solid MAO-supported catalysts

Complex	T (°C)	Time (minutes)	Activity (kg _{PE} /mol _{Zr} /h/bar)	M _w (kg/mol)	M _w /M _n
1_{sMAO}	50	30	4875 ± 412	694	2.8
	60	30	6755 ± 748	648	2.9
	70	30	6719 ± 194	562	3.1
	80	30	6013 ± 58	452	3.1
	90	30	5634 ± 86	392	3.1
	70	5	9145 ± 278	-	-
	70	15	8338 ± 746	-	-
	70	60	5981 ± 380	-	-
2_{sMAO}	50	30	5028 ± 580	654	2.9
	60	30	5550 ± 115	581	2.9
	70	30	5404 ± 117	520	3.0
	80	30	4943 ± 289	463	3.0
	90	30	4258 ± 115	456	3.1
	70	5	5244 ± 730	-	-
	70	15	5098 ± 77	-	-
	70	60	4611 ± 524	-	-
3_{sMAO}	50	30	4780 ± 142	693	2.9
	60	30	4826 ± 534	626	3.0
	70	30	5059 ± 0	535	3.2
	80	30	5042 ± 187	494	3.2
	90	30	4690 ± 16	429	3.3
	70	5	6356 ± 174	-	-
	70	15	4956 ± 903	-	-
	70	60	5879 ± 756	-	-
4_{sMAO}	50	30	4456 ± 716	778	3.0
	60	30	4963 ± 868	710	3.1
	70	30	4389 ± 506	687	3.3
	80	30	4090 ± 547	689	3.3
	90	30	2440 ± 10	536	3.5
	70	5	5282 ± 947	-	-
	70	15	6253 ± 1001	-	-
	70	60	3853 ± 452	-	-
5_{sMAO}	50	30	4378 ± 21	956	2.7
	60	30	5379 ± 112	673	2.9
	70	30	4312 ± 32	560	2.7
	80	30	4796 ± 205	376	2.6
	90	30	4305 ± 121	279	2.6
	70	5	7524 ± 268	-	-
	70	15	6163 ± 75	-	-
	70	60	4312 ± 31	-	-

Polymerisation conditions: 2 bar ethylene, 50 mL hexanes, 10 mg pre-catalyst, 150 mg TIBA.

5.5 Molecular weights

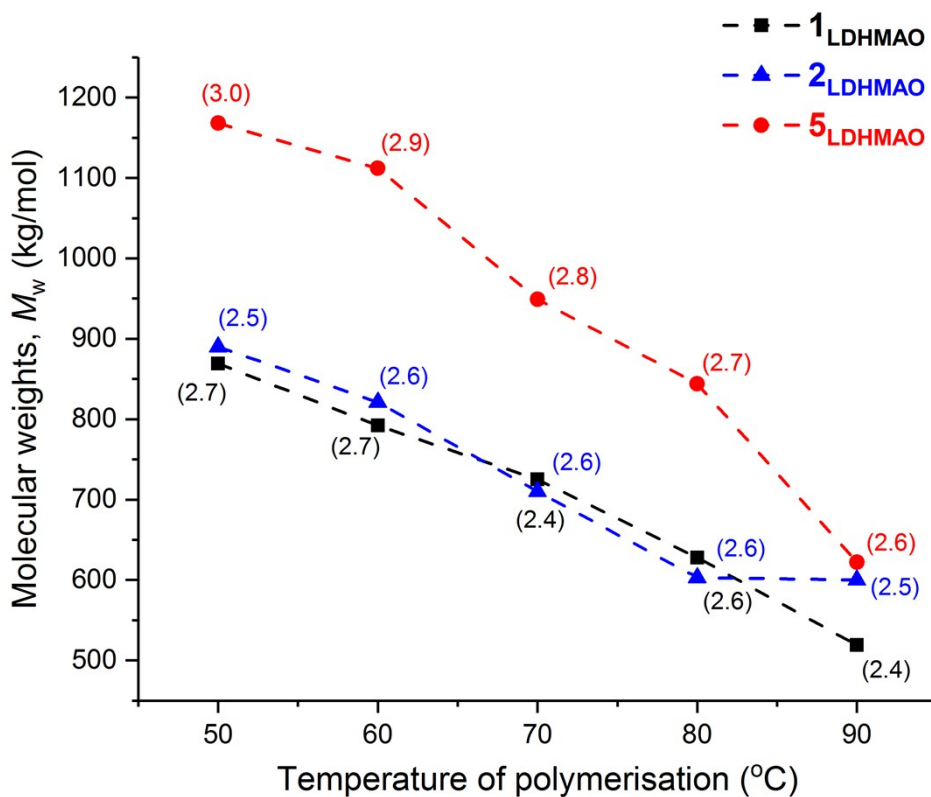


Fig. S43 Molecular weights, M_w , and polydispersities (M_w/M_n) in parentheses in function of temperature using LDHMAO- $\text{Me}_2\text{SB}(\text{tBu}_2\text{Flu}, \text{I}^*)\text{ZrCl}_2$ $\mathbf{1}_{\text{LDHMAO}}$ (black square), LDHMAO- $\text{Et}_2\text{SB}(\text{tBu}_2\text{Flu}, \text{I}^*)\text{ZrCl}_2$ $\mathbf{2}_{\text{LDHMAO}}$ (blue triangle) and LDHMAO- $\text{Me}_2\text{SB}(\text{tBu}_2\text{Flu}, \text{I}^*)\text{HfCl}_2$ $\mathbf{5}_{\text{LDHMAO}}$ (red circle). Polymerisation conditions: 2 bar ethylene, 50 mL hexanes, 10 mg pre-catalyst, 150 mg TIBA, 30 minutes.

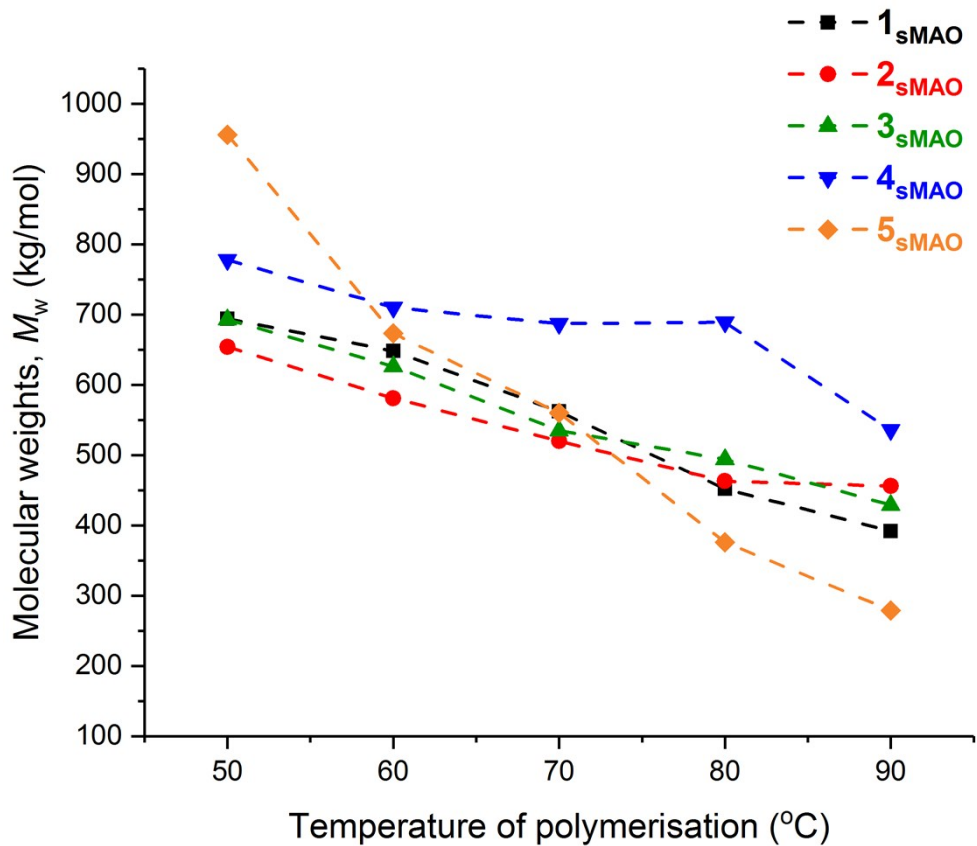


Fig. S44 Molecular weights, M_w , in function of temperature using sMAO- $\text{Me}_2\text{SB}(\text{tBu}_2\text{Flu}, \text{I}^*)\text{ZrCl}_2$ 1_{sMAO} (black square), sMAO- $\text{Et}_2\text{SB}(\text{tBu}_2\text{Flu}, \text{I}^*)\text{ZrCl}_2$ 2_{sMAO} (red circle), sMAO- $\text{MePropSB}(\text{tBu}_2\text{Flu}, \text{I}^*)\text{ZrCl}_2$ 3_{sMAO} (green triangle), sMAO- $\text{Me}_2\text{SB}(\text{tBu}_2\text{Flu}, {}^{3-\text{Et}}\text{I}^*)\text{ZrCl}_2$ 4_{sMAO} (blue down triangle) and sMAO- $\text{Me}_2\text{SB}(\text{tBu}_2\text{Flu}, \text{I}^*)\text{HfCl}_2$ 5_{sMAO} (red circle). Polymerisation conditions: 2 bar ethylene, 50 mL hexanes, 10 mg pre-catalyst, 150 mg TIBA, 30 minutes.

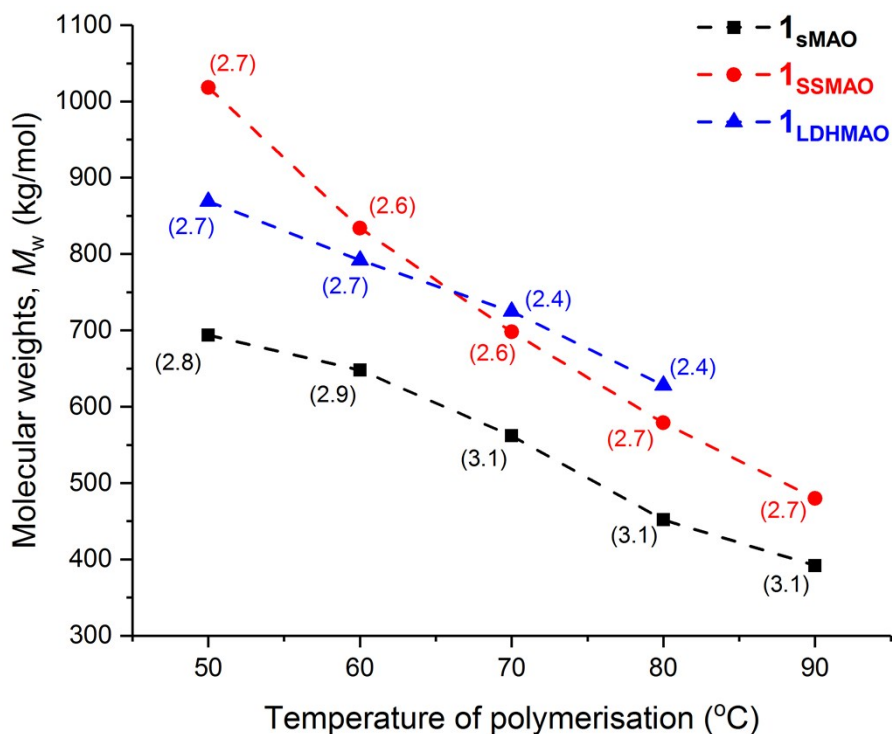


Fig. S45 Molecular weights, M_w , and polydispersities (M_w/M_n) in parentheses in function of temperature using sMAO- $\text{Me}_2\text{SB}(\text{tBu}_2\text{Flu}, \text{I}^*)\text{ZrCl}_2$ $\mathbf{1}_{\text{sMAO}}$ (black square), SSMAO- $\text{Me}_2\text{SB}(\text{tBu}_2\text{Flu}, \text{I}^*)\text{ZrCl}_2$ $\mathbf{1}_{\text{SSMAO}}$ (red circle), and LDHMAO- $\text{Me}_2\text{SB}(\text{tBu}_2\text{Flu}, \text{I}^*)\text{ZrCl}_2$ $\mathbf{1}_{\text{LDHMAO}}$ (blue triangle). Polymerisation conditions: 2 bar ethylene, 50 mL hexanes, 10 mg pre-catalyst, 150 mg TIBA, 30 minutes.

6. References

- (1) Cosier, J.; Glazer, A. M. *J. Appl. Crystallogr.* **1986**, *19*, 105.
- (2) Otwinowski, Z.; Minor, W. *Methods Enzymol.* **1997**, *276*, 307.
- (3) Blessing, R. H. *Acta Crystallogr. Sect. A* **1995**, *51*, 33.
- (4) Nowell, H.; Barnett, S. A.; Christensen, K. E.; Teat, S. J.; Allan, D. R. *J. Synchrotron Rad.* **2012**, *19*, 435.
- (5) Altomare, A.; Cascarano, G.; Giacovazzo, C.; Guagliardi, A.; Burla, M. C.; Polidori, G.; Camalli, M. *J. Appl. Crystallogr.* **1994**, *27*, 435.
- (6) Palatinus, L.; Chapuis, G. *J. Appl. Crystallogr.* **2007**, *40*, 786.
- (7) Betteridge, P. W.; Carruthers, J. R.; Cooper, R. I.; Prout, K.; Watkin, D. J. *J. Appl. Crystallogr.* **2003**, *36*, 1487.
- (8) (a) Cooper, R. I.; Thompson, A. L.; Watkin, D. J. *J. Appl. Crystallogr.* **2010**, *43*, 1100.
(b) Macrae, C. F.; Bruno, I. J.; Chisholm, J. A.; Edgington, P. R.; McCabe, P.; Pidcock, E.; Rodriguez-Monge, L.; Taylor, R.; Van De Streek, J.; Wood, P. A. *J. Appl. Crystallogr.* **2008**, *41*, 466.
- (9) L. J. Farrugia, *J. Appl. Crystallogr.* **1999**, *32*, 837.
- (10) Spek, A. L. *J. Appl. Crystallogr.* **2003**, *36*, 7.
- (11) Farrugia, L. J. *J. Appl. Crystallogr.* **2012**, *45*, 849.
- (12) Neese, F. Orca - an ab initio DFT and semi-empirical electronic structure package, 2011.
- (13) Kilpatrick, A. F. R.; Buffet, J.-C.; Noerby, P.; Rees, N. H.; Funnell, N. P.; Sripathongnak, S.; O'Hare, D. *Chem. Mater.* **2016**, *28*, 7444.
- (14) Kaji, E.; Yoshioka, E. US Patent 8,404,880 B2, **2013**.